

# **CHARACTERIZATION OF ELECTROLESS Ni-B-NANO TiO<sub>2</sub> COATING**

*Thesis presented in partial fulfillment of  
the requirement for the degree of*

***MASTER OF MECHANICAL ENGINEERING***

*By*

**AJOY KUMAR BHOWMICK**

Examination Roll Number: M4MEC23003

Registration Number: 72263 of 1998 - 1999

*UNDER THE GUIDANCE OF*

**Dr. Prasanta Sahoo**

**&**

**Dr. Tapan Kumar Barman**

**DEPARTMENT OF MECHANICAL ENGINEERING**

**FACULTY OF ENGINEERING AND TECHNOLOGY**

**JADAVPURUNIVERSITY**

**KOLKATA-700032**

**JUNE 2023**

### **CERTIFICATE OF APPROVAL\***

This foregoing thesis is hereby accepted and approved as a legitimate study into an engineering subject that was carried out and presented in a way that justifies its acceptance as a requirement for the degree for which it has been submitted. It is understood that by signing this approval, the signatories are simply endorsing the thesis for the purpose for which it has been submitted and are not endorsing or endorsing any statements made, opinions offered, or conclusions reached therein.

**Committee**

**On Final Examination for**

**Evaluation of the Thesis**

---

---

---

**\* If the thesis is accepted, only.**

## **FACULTY OF ENGINEERING AND TECHNOLOGY JADAVPUR UNIVERSITY**

We here by recommend that the thesis presented under our supervision by **Mr. Ajoy Kumar Bhowmick** entitled “**Characterization Of Electroless Ni-B-Nano TiO<sub>2</sub> Coating.**” be accepted in partial fulfillment of the requirements for the degree of Master of Mechanical Engineering.

**Countersigned**

-----

-----

-----

**Thesis Advisors**

-----

**Head of the Department  
Mechanical Engineering**

-----

**Dean of Faculty of  
Engineering and Technology**

## ACKNOWLEDGEMENT

---

I do feel lucky enough and grateful to God that I got a chance to work under **the eminent scientists, Dr. Prasanta Sahoo** who transformed my attitude towards the goal of my master degree concept to the passion of study no sooner he made me believe to think about the measurement of clouds. I am grateful to **Dr. Tapan Kumar Barman** whose constant pressure and inspiration obliged me to move ahead keeping aside all my constraints. My special thanks to **Mr. Deviprassana Mohanty** (Ph.D. Scholar) who helped me a lot to learn about my experiments. Their immense knowledge enabled me to complete my thesis.

I would like to thank to the Centre Of Excellence in Advanced Materials, **National Institute Of Technology, Durgapur** for providing me the SEM results of composite coating, Department of **Mechanical Engineering, KGP IIT** for XRD and Central Research Faculty, **Indian Institute of Engineering Science and Technology, Shibpur** for providing the SEM results of tribo tested composite coatings.

I must convey my regards to **Dr. Suman Kalyan Das**, Laboratory-in-charge of Machine Elements Laboratory who helped me a lot for pursuing my experiments in the Lab. The environment of Machine Elements Lab makes me so happy to think of it as a second home and all the senior research scholars are so cooperative to work in that home. An inspiring smile by the professors like **Dr. Anirban Mitra , Dr. Souvik Ghosh** made me energetic often to work harder in that home.

I must keep silent about the role of my wife **Piyali Bhowmick**, as no word is sufficient to judge about the level of her constant sacrifice.... the precious gem left for me in the world from both of my fathers.

Date:

-----  
(AJAY KUMAR BHOWMICK)

# CONTENTS

---

	<i>PAGE NO.</i>
<b>CERTIFICATE OF APPROVAL</b>	ii
<b>CERTIFICATE OF SUPERVISORS</b>	iii
<b>ACKNOWLEDGEMENT</b>	iv
<b>CONTENTS</b>	v
<b>LIST OF FIGURES</b>	viii
<b>LIST OF TABLES</b>	xi
 <b>CHAPTER 1: INTRODUCTION</b>	
 1.1 INTRODUCTION	01
1.2 ADVANTAGES AND DISADVANTAGES OF ELECTROLESS NICKEL (EN) COATING	03
1.3 APPLICATIONS OF ELECTROLESS COATING	04
1.4 CLASSIFICATION OF ELECTROLESS NICKEL COATING	06
1.4.1 Alloy and poly-alloy coating	07
1.4.2 Composite coating	07
1.4.3 Metallic coatings	08
1.5 FUNDAMENTALS OF ELECTROLESS NICKEL COATING	08
1.6 EFFECT OF PROCESS PARAMETERS ON ELECTROLESS NICKEL-BORON COMPOSITE COATING	09
1.6.1 Effect of reducing agent	14
(i) DMAB or dimethylamineborane (C <sub>2</sub> H <sub>7</sub> BN)	15
(ii) Sodium borohydride (NaBH <sub>4</sub> )	15
1.6.2 Effect of complexing agent	16
1.6.3 Effect of temperature	17

1.6.4	Effect of pH value	18
1.6.5	Effect of time	19
1.6.6	Effect of surfactant	19
1.6.7	Effect of stabilizers	20
1.6.8	Effect of buffering agents	20
1.6.9	Effect of heat treatment	20
1.7	LITERATURE REVIEW	22
1.7.1	Tribological studies of electroless nickel boron tinania (Ni-B-TiO <sub>2</sub> ) coating	26
1.7.2	Micro structural, thermal and chemical studies	28
1.7.3	Deposit hardness	30
1.7.4	Summery of literature review	30
1.8	PRESENT WORK	31
1.9	PRESENT THESIS	32

## **CHAPTER 2: EXPERIMENTAL METHODS**

2.1	INTRODUCTION	33
2.2	DEPOSITION OF ELECTROLESS NICKEL BORON TITANIA (Ni-B-TiO <sub>2</sub> ) COATING	34
2.2.1	Preparation of substrate	34
2.2.2	Preparation of bath	34
2.2.3	Steps for the Deposition Process	35
2.3	MICROSTRUCTURE AND COMPOUND ANALYSIS	37
2.4	SCARTCH TEST	39
2.5	ELECTRO CHEMICAL CORROSION	40
2.6	FRICTION AND WEAR TESTS	42
2.6.1	Equipment used	42
2.6.2	Selection of process parameters	43

2.6.3 Response variables	44
2.6.4 Design of experiments	45
2.6.5 Analysis of variance	46
<b>CHAPTER 3: RESULTS &amp; DISCUSSIONS</b>	
3.1 INTRODUCTION	47
3.2 RESULTS AND DISCUSSION	47
3.2.1 Surface morphology	47
3.2.2 Friction and wear under dry condition	49
3.2.2.1 Analysis of variance (ANOVA) for wear	50
3.2.2.2 Analysis of signal to noise ratio for wear	52
3.2.2.3 Analysis of variance (ANOVA) for friction	54
3.2.2.4 Analysis of signal to noise ratio for friction	55
3.2.3 Microstructural Analysis	56
3.2.4 Post tribo test surface morphology analysis	58
3.2.5 Scratch test	59
3.2.6 Corrosion test	61
3.2.7 Analysis of composition	64
<b>CHAPTER 4: CONCLUSIONS AND FUTURE SCOPE OF WORK</b>	
4.1 CONCLUSION	65
4.2 FUTURE SCOPE OF WORK	66
<b>REFERENCES</b>	68
<b>PUBLICATION</b>	76

## LIST OF FIGURES

	PAGE NO.	
1. <b>Fig. 1.1</b> Different types of surface treatment and benefits of composite coating	02	
2. <b>Fig. 1.2</b> Application of electroless nickel (Ni) coating	05	
3. <b>Fig. 1.3</b> Comparison between immersion deposition and electroless deposition in respect of deposit thickness vs. time .	11	
4. <b>Fig. 1.4</b> Schematic representation of an electroless coating system	12	
5. <b>Fig. 1.5</b> The hardness of Ni-B coatings is influenced by the temperature of the heat treatment	22	
6. <b>Fig. 1.6</b> Scratches traces: (a) Ni-B coating (b) Ni-B-TiO <sub>2</sub> composite coating @ indenter tip radius 200mm. (c) scratch test: @ indenter tip radius 100mm in progressive load .	27	
7. <b>Fig. 1.7</b> Characteristic part of the XRD power pattern of the TiO <sub>2</sub> sample and its thermal deposition products A <sub>1</sub> (150°C), A <sub>2</sub> (300°C), A <sub>5</sub> (1000°C).	29	
8. <b>Fig. 1.8</b> TGA and differential thermal analysis i.e. DTA on TiO <sub>2</sub> (stabilized with polyethylene glycol or PEG) @ heat rate 10 <sup>0</sup> C per minute .	29	
9. <b>Fig. 1.9</b> Comparison of hardness as well as thickness values for different coatings like Ni, Ni-B (1.84% Boron) and Ni(Sm) films	30	
10. <b>Fig. 2.1</b> Flow chart: experimental methods and procedure	33	
11. <b>Fig. 2.2</b> Electroless Bath of Ni-B-TiO <sub>2</sub> composite coating (JU M/C Elements Laboratory)	36	
12. <b>Fig. 2.3</b> SEM M/C1 [FESEM ZEISS, * potential - 20 kV * working distance - 9.5 mm.], National Institute of Technology, Durgapur.	37	vii



13.	<b>Fig. 2.4</b> Scanning electron microscope (SEM2), make: HITACHI, model: S-3400N, IEST, Shibpur.	38
14.	<b>Fig. 2.5</b> D-8 advanced X-Ray diffraction machine , National Institute of Technology , Durgapur	39
15.	<b>Fig. 2.6</b> Scratch tester (TR-101-IAS), JU M/C Elements Laboratory	40
16.	<b>Fig. 2.7</b> Potentiostat from ACM Instruments Gill AC, UK	41
17.	<b>Fig. 2.8</b> Schematic view of corrosion testing process diagram	41
18.	<b>Fig. 2.9</b> POD (Pin-on-disk) tribological tester (Model: TR-208-M2, Make: DUCOM)	43
19.	<b>Fig. 2.10</b> Process response control diagram	44
20.	<b>Fig. 3.1</b> SEM results: surface structure (morphologies) of (i) Ni-B Alloy surface: (a) and (b); cross section : (c) and (d) (ii) Ni-B-TiO <sub>2</sub> composite coating surface (e) and (f) ; cross section (g) and (h) having different magnification.	48
21.	<b>Fig. 3.2</b> SEM results: images of Ni-B and Ni-B-TiO <sub>2</sub> coating at different magnification 1000X and 5000X).	49
22.	<b>Fig. 3.3</b> Analysis of variance (ANOVA) for wear	51
23.	<b>Fig. 3.4</b> Interaction plot of all four tribological parameters (Nano %-Load-Speed-Sliding Distance) for wear.	52
24.	<b>Fig. 3.5</b> Signal to noise ratio for wear	53
25.	<b>Fig. 3.6</b> Analysis of variance (ANOVA) for COF	54
26.	<b>Fig. 3.7</b> Interaction plot of all four tribological parameters (Nano %-Load-Speed-Sliding Distance) for COF	55
27.	<b>Fig. 3.8</b> Signal to noise ratio for COF	56
28.	<b>Fig. 3.9</b> SEM imaging: (a) deposited Ni-B coating (b) Ni-B-TiO <sub>2</sub> (1 gm per liter)	57

<b>29. Fig. 3.10</b>	Nickel-Boron-TiO <sub>2</sub> deposition elemental distribution as seen by EDAX region scans.	57
<b>30. Fig. 3.11</b>	Post tribo test crack structure: crack arrests as nano particles increases in (a), (b),(c) respectively.	58
<b>31. Fig. 3.12</b>	(a),(b) Surface morphology before tribo test Ni-B as well as Ni-B-TiO <sub>2</sub> composite. (c),(d) surface morphology after tribo test Ni-B-TiO <sub>2</sub> composite with load 20N and 5 N respectively	58
<b>32. Fig. 3.13</b>	Scratch optical images: (a) nickel boron (Ni-B) and (b) Ni-B-TiO <sub>2</sub> composite coatings experimented at a load of 30 newton, stroke length of 5 mm and scratch speed of 0.1 mm per second.	59
<b>33. Fig. 3.14</b>	Bar graph: scratch resistance (/hardness) of Ni-B and Ni-B-TiO <sub>2</sub> at various loads.	60
<b>34. Fig. 3.15</b>	Tafel curve: in favor of deposited specimen.	61
<b>34. Fig. 3.16</b>	Nyquist plot shown in different colour for Ni-B and Ni-B-TiO <sub>2</sub> coatings.	62
<b>35. Fig. 3.17</b>	EDX for Ni-B coating spectrum (a) in applied deposition and (b) in heat treated (annealed at 350 <sup>0</sup> C for 1hr).	63
<b>36. Fig. 3.18</b>	EDAX spectra for Ni-B-TiO <sub>2</sub> coatings	64

## LIST OF TABLES

---

	<i>PAGE NO.</i>
1. Table 1.1 Applications of electroless Nickel-B coating	05
2. Table 1.2 Electroless bath components and their roles	11
3. Table 1.3 Different reducing agent for different electroless nickel (EN) plating	15
4. Table 1.4 Change of pH value on solution and deposition	19
5. Table 1.5 Common electroless nickel coating bath applications, operating circumstances, and component types	23
6. Table 1.6 Micro hardness, elastic modulus, grain size and roughness	27
7. Table 2.1 Composition of bath	35
8. Table 2.2 Design variables and their levels	43
9. Table 2.3 Taguchi analysis (L16)	46
10. Table 3.1 Results from experiments measuring friction coefficient and weight loss at dry condition	50
11. Table 3.2 ANOVA analysis for wear characteristic	52
12. Table 3.3 ANOVA analysis for friction characteristic	55
13. Table 3.4 Corrosion results derived from the given tafel curves and nyquist plots	63

# INTRODUCTION

*This chapter provides the introduction to electroless coating and an extensive literature review to set the goal of the present study of electroless coating with nano particles.*

## 1.1 INTRODUCTION

We all know that Tribology is best described as the science and technology of interacting surfaces in relative motion, which includes the study of friction, wear, and lubrication. So understanding of tribological principles is essential to the proper design of machine components which leads almost every aspects of our daily life directly or indirectly through the socio-economic parameters. An extensive analysis that took into account the four major energy-consuming sectors— electricity production, transportation, residential and manufacturing —calculated the effect of friction and wear on energy use, economic output, and CO<sub>2</sub> emissions on a global level. According to the report by Holmberg and Erdemir (2017), in total, ~23% (119 EJ) of the world's total energy consumption originates from tribological contacts. Of that 20% (103 EJ) is used to overcome friction and 3% (16 EJ) is used to re-manufacture worn parts and spare equipment due to wear and wear related failures. It also looks into how new surfaces, material, and lubrication technologies can be used in machinery, automobiles and other equipment all over the world to potentially reduce energy losses caused by friction and wear by 40% over the long term i.e. for 15 years and by 18% over the short term i.e. 8 years. On a worldwide scale, this cost savings would equate to 8.7% of long-term energy use and 1.4% of yearly GDP [Holmberg and Erdemir, 2017].

The surface of a material is strengthened due to plastic deformations. When a material is deformed plastically more dislocations are formed which impedes further movement which leads to increase in strength of materials. Micro machining, polishing, grinding, and shot peening are conventional mechanical surface modification techniques that entail physically modifying, or removing material from the surface. Achieving certain surface roughness and topographies, removing contaminants from surface, and enhancing adhesion are the primary goals of mechanical modification. These techniques are usually used in combination with other procedures as they solely cannot completely improve the surface properties of the

material. Hard surface coatings are particularly useful in this situation due to their superior tribological characteristics.

Thermal spraying is a broad terminology for a coating process in which materials are deposited in a spray of finely distributed liquefied or semi liquefied particulates to build layered deposition coatings. Sathish et al. (2022), in Fig. 1.1, depict different types of surface treatment and benefits of composite coating vividly. Duplex and composite coatings can be utilized in the thermal spray technique to enhance the tribological properties of a broad range of engineering materials while saving money; service life extension, maintenance expenses, and replacement costs are lower than for single layered coatings.

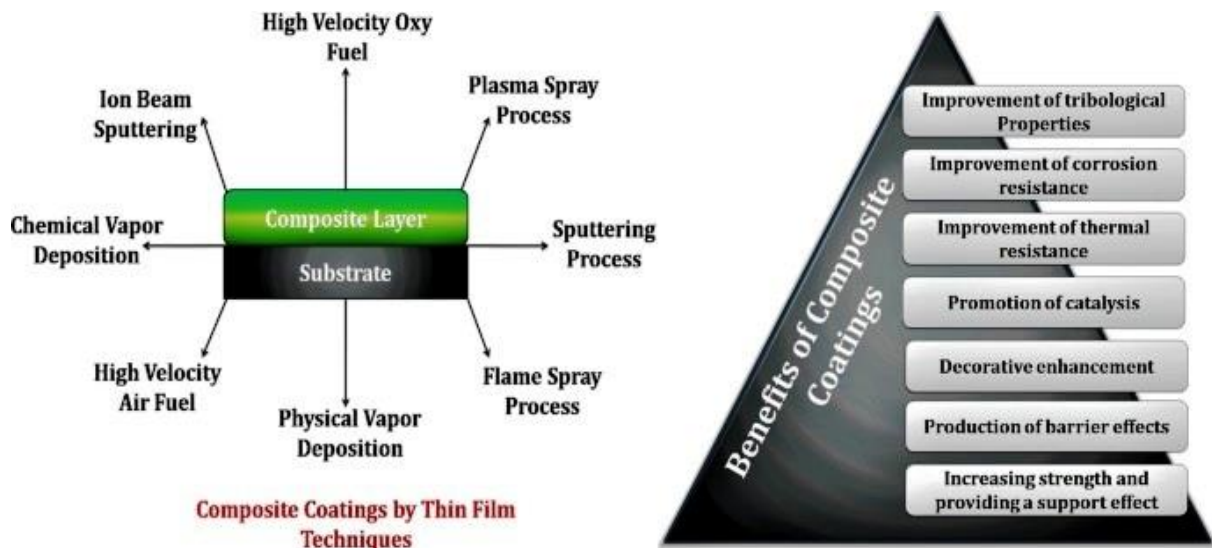


**Fig. 1.1** Different types of surface treatment and benefits of composite coating (Sathish et al. 2022).

Optimization technique played a major role to improve the materials. For instances instead of making a whole body by titania it is more cost effective to make a layer of coatings over the mild steel material to get almost same mechanical property. Different type of coatings like powder coating, epoxy coating developed in sequence of their necessities. By using a reducing chemical bath today we can deposit metals like copper, nickel, silver, gold, or palladium on the surface of a variety of materials by electroless coatings method. But these

coatings were first found in the year 1994 by Mr. Grace E. Riddell and Mr. Abner Brenner. During the last few decades after this invention, coating process improved in several ways and now a days incorporation of nano particles along with different processes including heat treatment process, exhibits high mechanical properties and supports high industrial demands. Researcher's interest in developing metal deposition technologies based on electroless nickel, alloy and other composite coatings on various surfaces has increased as a result of several great features that have recently enabled numerous applications. These coatings have recently demonstrated significant wear and corrosion resistant qualities and much more recent advancement have become crucial for applications ranging from macro to nanoscale [Sudagar et al. 2013].

## **1.2 ADVANTAGES AND DISADVANTAGE OF ELECTROLESS NICKEL (EN) COATING**

**The main advantages of electroless Nickel coatings are:**

- 1 Resistance to wear and corrosion.
- 2 Increases in micro hardness.
- 3 Increase thermal-resistance.
- 4 Regardless of the substrates' geometry, the deposit is even and smooth.
- 5 Oxidation resistance.
- 6 Good solder-ability, bond-ability and weld-ability properties.
- 7 Greater lubricity.
- 8 Nonmagnetic properties of high-phosphorus nickel alloy.
- 9 Good appearance and brightness.
- 10 Low co-efficient of thermal expansion and high thermal conductivity.
- 11 Good chemical stability.

**The main disadvantages of electroless nickel coatings are:**

- a. Lifespan of chemicals is limited.
- b. Waste treatment cost is high due to the speedy chemical renewal.

### **1.3 APPLICATIONS OF ELECTROLESS NICKEL COATING**

The coating processes that use aqueous solutions (electroplating as well as electroless plating) have recently attracted a lot of attention due to their special advantages, for example easier coating process, very low cost, enough deposition rate, formation of an even coating layers and promising mechanical properties, high hardness, nice wear resistance, and huge anti-corrosion properties. The electroless nickel coating process, one of the aqueous solution metal deposition techniques is better known and has undergone notable changes since it was developed by Brenner and Riddell 1946. This process consist of a unique set of characteristics, including uniform material thickness, high value of hardness, excellent wear as well as abrasion resistance, very good solderability, amorphous as well as microcrystalline-deposits, low frictional coefficients, good reflectivity, lower resistivity, and very good magnetic properties, among others. For changing the surface characteristics of numerous materials, including non-conducting materials like plastics and metals like steel, aluminum, and copper, electroless nickel deposition has gained economic significance [Cheong et al. 2007]. Electroless coatings are used in various industries including Micro-electromechanical Systems (MEMS), electromagnetic interference (EMI), reactor membranes, heat exchangers, powder metallurgy and the reduction of bacterial adhesion. When compared to the electro deposition technique, the electroless coating process has the outstanding advantage of thickness homogeneity [Afroukhteh et al. 2012]. When considering the obvious benefits of boron and the possible benefits of electroless coating technique, improving surface characteristics by depositing Nickel-Boron (Ni-B) coating through electroless coating process can be regarded as a good alternative. Due to its maturity, scalability, and reproducibility, the Ni-B electroless coating technique was selected as a method for bulk production in the year 1989. Since then the electroless Nickel-Boron (Ni-B) coating technique has drawn a lot of interest for its ability to enhance the surface characteristics of a wide range of substrates [Vitry et al. 2012]. The homogeneous coatings created by the electroless Nickel-Boron (Ni-B) coating method contain a significant quantity of nickel boride, which significantly improves their wear and abrasion qualities. The use of carbon steels, iron, stainless steels, aluminum and aluminum alloys, plastics and other substrate materials is possible. High hardness (above that of tool steels), extreme wear resistance (superior than hard material of chromium coatings), and promising corrosion-resistant qualities (Nickel Phosphorous coatings) are only a few of the exceptional

advantages of electroless Nickel-Boron (Ni-B) coatings. Electroless Nickel Boron (Ni-B) coatings have additional benefits in addition to the ones already mentioned, such as marginal cost, maximum wear resistance, even thickness, fare lubricity, very good ductility and marvelous corrosion resistance, very nice solderability, inflated electrical properties, small porosity, good bonding, high conductivity, and exceptional electro-magnetic properties [Bülbül et al.2016]. Electroless coatings are widely employed in all types of sectors because to their many benefits. Sayyad & Senanayake (2021), depict different use of of Electroless Nickel (Ni) coating in Fig. 1.2.

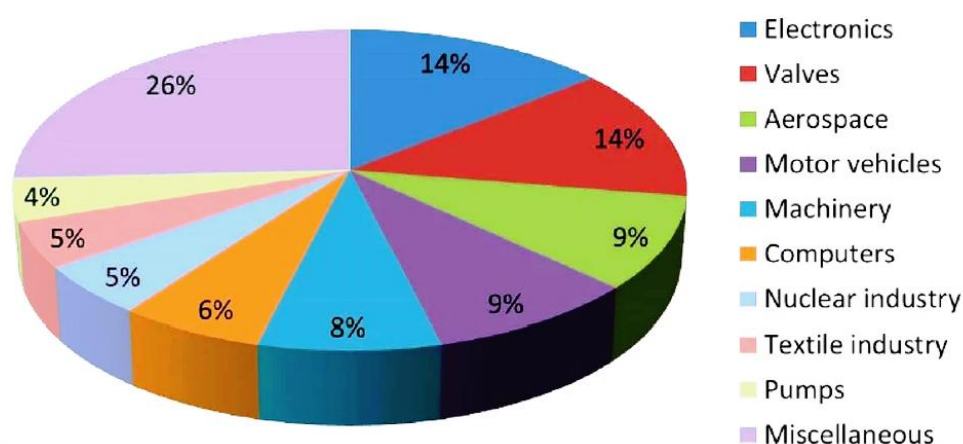


**Fig. 1.2** Application of electroless nickel (Ni) coating (Sayyad and Senanayake,2021).

There is a wide range of applications of electroless Nickel coating. A review has been made by Agarwala and Agarwala,2003 and depending upon the coating thickness they may be tabulated in the Table 1.1.

**Table 1.1** Applications of electroless Nickel-B coating

Application Areas	Thickness of Coating (in micrometer)	Components
Automobile Industry	2–38	turbochargers, carburetor parts, transmission parts, fuel injection, gears, hose couplings, exhaust valve disc brake pistons, ignition systems etc.



Air craft/ Aerospace	10–50	servo valves, sensors, electronic switch gear compressor blades, safety devices, pistons heads, engine main shafts and propellers, hydraulic actuator splines, seal snaps and spacers, landing gear components, pilot tables, oil nozzle components, flanges, universal joints, feed tubes for engine oil.
Chemical & Petroleum	25-125	Pressure vessels, impeller, discharge manifold, Inlet nozzle , Gate valve, spray nozzle, pump, drilling pump, hydraulic actuator, Down hole pipe, plunger, turbine, Swing checking valve, Subterranean-Pipe etc.
Electrical Parts	12–25	Rotor and stator components, shaft of motor etc.
Electronic Parts	2–25	PCB, transistor cans Head sinks, mother board, semiconductor, MEMS, Capacitors, LEDs, Wafers, Batteries, sensors etc.
Food Process Unit	12–25	Freezer, mixing louts, and feed screw and extruders,Gravy Machine, baking pans, Snack Food Extruder, Food Mixer, Food Extruders etc.
Marine Engineering	25–50	Different type of pumps, vessels and its equipment.
Handling Materials	12–75	Gear drive, belt drive , pulley, shaft, break , clutch, etc.
Medical and Pharmaceutical	12–25	Stents, Hearing devices, Cable assemblies, Needlesdifferent surgical instrument, size ring equipment etc.
Defense Unit	8–75	Fasteners, Gun barrels, Screws, Detonators, Fasteners, Missile components, Shields, Radar arrays, radar equipment etc.
Mining Industry	30–60	Excavator parts , pneumatic jack , rock driller, Hydraulic actuators, boomers etc.
Wood and craft	~30	Saw blades, drill machine, knife holders etc.

## 1.4 CLASSIFICATION OF ELECTROLESS NICKEL COATING

Electroless nickel coatings vary widely from one another. Depending on the end-use requirement, many varieties have been designed to provide particular features. Pure nickel coating, nickel alloy coating, and nickel composite coating are the three different types of EN coatings. Alkaline ( $\geq \text{pH } 7$ ) /acidic baths containing sodium hypophosphite, sodium borohydride, and aminoborane as reducing-agents can be used to create nickel alloy and composite coatings.

#### **1.4.1 Alloy and poly-alloy coating:**

In addition to plating via reduction reaction, two further processes also recorded. These processes include immersion plating on steel utilizing nickel chloride ( $\text{NiCl}_2$ ) and boric acid ( $\text{H}_3\text{BO}_3$ ) solutions as well as the breakdown of nickel carbonyl vapor on a steel substrate. However, the former is less protective and weakly adhered, while the latter is dangerous. Utilizing the autocatalytic reduction reaction has the benefit of preserving overall homogeneity of coating in context of constituents and thickness, regardless of substrate depth fluctuations. There have been deposits of a number of binary and ternary alloys, including studies of Ni-P [Brenner and Riddell, 1946].

To achieve the appropriate mechanical and physical qualities, several alloys are coated. The element with the most widespread phosphorous coating is nickel, which is surprising.

In addition to nickel, most of the alloys also contain one or more of the following components: Cobalt (Co), Platinum (Pt), Copper (Cu), Silver (Ag) etc. These alloys have exceptional properties.

Many electroless nickel plating processes result in deposits with three or four components. There are several of them, such as Nickel-Iron Alloys, Nickel-Molybdenum Alloys, Nickel-Copper-Alloys, Nickel Chromium Iron Alloys, Nickel-Chromium-Molybdenum Alloys, Nickel Chromium Cobalt Alloys and Nickel-Titania Alloys etc. Each of the abovementioned elements is created to maximize features including plastic deformation resistance, high heat resistance, improved Electrical resistivity and conductivity as well as magnetic properties.

#### **1.4.2 Composite coating:**

Particulate matter and electroless nickel coatings have been co-deposited since the 1960s. In an effort to increase the corrosion-resistance of Ni-Cr or Ni-Fe-Cr electro-deposits, it was used an in-between layer made up of PVC and  $\text{Al}_2\text{O}_3$  particles that were evenly dispersed throughout a metallic matrix. Electroless coating was used to deposit this intermediary layer. Since then, other techniques have been employed to produce composite Ni-P- $\text{Al}_2\text{O}_3$  coatings. Strong grain of carbides, ceramics, and oxides are the example. More recent ones include Ni-P-  $\text{Al}_2\text{O}_3$ - $\text{ZrO}_2$  and composite coatings made of silver and graphite. Dust of poly-

tetrafluoroethylene(PTFE), fluorinated carbon (CF<sub>x</sub>) etc. may be considered as the soft particles.

Recently, composite coatings made of nickel('Ni'), boron('B'), and a few additional elements have also been described; these coatings are used as 'light emitting coatings'. Co-deposition success is dependent on a number of variables, including particle size distribution, inert-nature or catalytic, composition of the bath, and compatibility of the dispersions with the metal matrix. By hanging graphite-particles in the electroless plating (EN) bath, graphite can be added to silver coatings. DMAB, sodium hydroxide, sodium cyanide, silver cyanide, and thiourea are all ingredients in the plating bath. Typically, the temperature employed is around 70°C. The traditional reduction reaction procedure with particle suspensions is used in electroless composite coating. Particle characterization [Agarwala and Agarwala 2003], bath chemistry, operation conditions, and other variables can all affect the co-deposition of particles immersion in deposits of electroless coatings.

#### **1.4.3 Metallic coatings:**

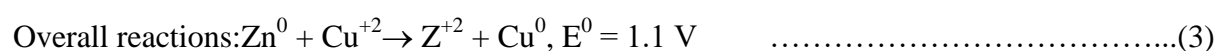
Electroless copper coatings are used before the electroplating on different type of protector materials (those are not a good conduction properties) like ceramic, plastic, polymer etc.

Electronic device shielding can also be accomplished with electroless copper covering. These coatings typically range in thickness from 12µm to 30 µm. The plating-bath contains different reducing agent, complexing agent, stabilizer including metal-ions. Copper ions can be obtained from copper sulphates, acetates, or nitrates. Formaldehyde is the common reducing-agent, but others, such as sodium hypophosphite and DMAB, can also be utilized. Common complexing agents include potassium titrate and sodium hydroxide. As bath stabilizers, vanadium oxide or thiourea are employed. The bath can be used to apply the composite coating at any temperature between room temperature and 70°C. To get bright coatings, the pH is required to maintain at the levels of approx. 12, though the plating-bath is much stable at around pH of approximately 9.

### **1.5 FUNDAMENTALS OF ELECTROLESS NICKEL COATING**

An electrochemical mechanism, including oxidation as well as reduction (redox), reactions involving the transfer of electrons between reacting chemical species, is involved in the chemical deposition of the metal from the aqueous solution of the salt of the metal in

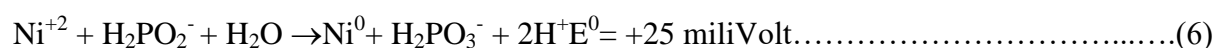
consideration. While reduction is recognized by an increase in electrons, oxidation of a material is represented by losing of electrons. Additionally, depletion denotes the cathodic activity, whereas oxidation specifies an anodic reaction. The metal displacement reaction is the most fundamental type of chemical plating. For instance, as the zinc(Zn) metal is submerged in the solution of copper sulphate ( $\text{CuSO}_4$ ), the less noble zinc(Zn) metal atoms dissolved and are subsequently replaced by copper(Cu) atoms from the aqueous solution. Subsequent reactions can be shown as follows:



The zinc substrate's surface transforms into a mosaic of anodic (zinc) and cathode (copper) sides no sooner the displacement reaction begins. When copper has almost completely covered the substrate, the displacement operation is repeated. At this stage, copper deposition ends and the zinc anode's oxidation (dissolution) almost completely stops.

Displacement plating using chemicals results in deposits that are only a few microns thick, often between 1 and 3  $\mu\text{m}$ . There are limited applications for chemical plating using the displacement technique. It is crucial to use a sustainable oxidation reaction instead of dissolving the substrate in order to continuously create thick coatings chemically without consuming the substrate. The substrate must initially serve as the sole site of the deposition reaction, and subsequent deposits must be made on top of the first deposit. Compared to the redox potential of a metal being deposited through immersion, this chemical process often has a higher positive redox potential.

Without affecting the mass of the substrate, the chemical-deposition of nickel metal using hypophosphite satisfies the oxidation as well as redox potential criteria:



The oxidation and reduction equations are added together in this. Due to the presence of hydrogen evolution during EN deposition, these reactions do not accurately depict the electroless plating reaction. Fig.1.3 shows the comparison between immersion deposition and electroless deposition in respect of deposit thickness vs. time (Mallory and Hajdu, 1990). Brenner and Riddell used the phrase "electroless plating" to refer to a method for plating nickel or cobalt alloys on metal surfaces without the use of an external source of electricity.

The phrase has since been expanded to cover any procedure that constantly deposits metal from the aqueous solution over time. The primary characteristic of electroless plating is the special reduction of metal ions solely at the surface of a catalytic-substrate immersed in the solution of those metal ions, with subsequent deposition on the substrate occurring as a result of the deposit's catalytic action. Since the deposit catalysis the reduction reaction, the plating process is also referred to as "autocatalytic". By Wurtz (1845) it was noted that hypophosphite anions decreased nickel cations in 1844. Wurtz, however, only managed to get some black powder. Breteau discovered the first shiny metallic deposits of nickel phosphorus (Ni-P) alloys in 1911 (Mirza et al. 2016). In 1916, Roux received the first patent for an electroless nickel plating bath (Duncan 1993).

However, these type baths spontaneously broke down and left behind deposits on whatever surface they came into touch with, including the container's sides. Other researchers looked at the procedure, but they were more concerned with the chemical reaction than with the plating procedure. A publication in 1946, by Brenner and Riddell (1946) outlined the ideal circumstances for achieving the above-described electroless deposition. The procedure has been extensively researched and developed by numerous individuals throughout the years to reach its current stage of development. Comparison between immersion deposition and electroless deposition in respect of deposit thickness vs. time has been shown in Fig.1.3 (Mallory and Haju, 1990).

Unlike electroplating, which needs rectifiers, electrical current, and anodes, EN does not. Metal ion, complexing agent, a reducing-agent and buffering agents, stabilizers, and an aqueous solution are all present during the deposition process.

A nickel alloy is deposited as per the result of chemical processes occurring on the surface of the component being plated. An electroless bath typically consists of a metal ion source, a reducing-agent, stabilizer, complexing agent, buffering-agent, and surfactant. It also functions within a specific pH and temperature range. The role of each component is summarized in Table 1.2 given below:

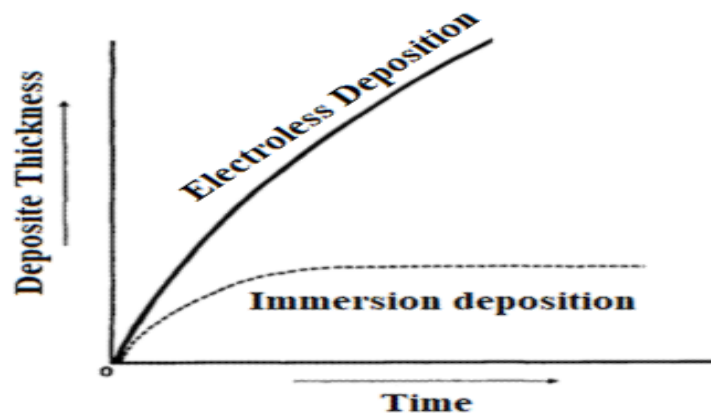


**Fig. 1.3** Comparison between immersion deposition and electroless deposition in respect of deposit thickness vs. time [Mallory and Haju, 1990].

**Table 1.2** Electroless bath components and their roles (Brenner and Riddell 991).

Components	Function	Example
Nickel(Ni) ions	metal source	Nickel Chloride( $\text{NiCl}_2$ ), Nickel Acetate ( $\text{C}_4\text{H}_6\text{NiO}_4$ ), Nickel Sulphate ( $\text{NiSO}_4$ )
Reducing(Electron donner) Agents	Supply of electrons to reduce the metal ions	Sodium Hypo phosphite ( $\text{NaPO}_2\text{H}_2$ ) Sodium Boro hydride Hydrazine ( $\text{NaBH}_4$ )
Complexant Agents	Resist surplus nickel ion immersion	Monocarboxylic Acids Dicarboxylic Acids Hydroxycarboxylic Acids
Accelerators	Activate the reducing agent and Increase deposition	Anions of some mono and di Carboxylic acids, Fluorides
Stabilizers	Preventsolutionbreakdownbyshieldingcatalyticallyactivedeposition	Lead, Tin, Arsenic, Molybdenum, Cadmium or Thalliumions
Buffers	To control pH(acidity or alkalinity)	Cobalt salt( $\text{CoCl}_2$ ) to water( $\text{H}_2\text{O}$ )
pH Controller	For succeeding pH adjustment	Sulphuric ( $\text{H}_2\text{SO}_4$ ), Hydrochloric ( $\text{HCl}$ ) acids, Causticsoda ( $\text{NaOH}$ ), Ammonia( $\text{NH}_3$ )
Wetting Agents	Increase wettability of surfaces to be Coated	Ionic Nonionic surfactants

The coating created by the electroless deposition technique has improved mechanical and tribological properties, but controlling the stability of the electroless bath is challenging, which is a drawback of the process. Since the technique's inception, there has been a surge in research into as well as development of newer coatings based on the electroless method to meet the needs of the current industrial demands. The electroless deposition set up has been depicted in Fig 1.4. This method makes it simple to cover challenging substrates and can plate a variety of metals. Though this method is mainly associated with hypophosphite reduced electroless Ni-P coating (Panja and Sahoo, 2014) and borohydride reduced Ni-B coating (Das and Sahoo 2011) and their composite as well as poly alloy coatings (Agarwala and Agarwala, 2003).

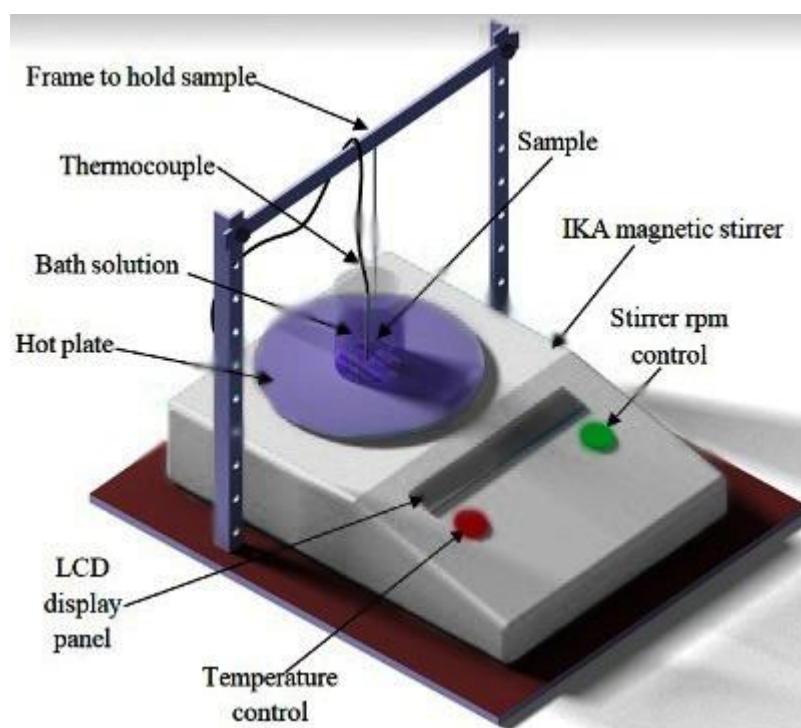


**Fig. 1.4** Schematic representation of an electroless coating system

Since the beginning of the 1980s, EN coatings have been utilized more often in a variety of sectors. Superior corrosion as well as wear resistance, remarkably uniformity, a variety range of thicknesses, a variety of mechanical as well as physical properties, exceptional solder ability and surface lubricity (Sudagar et al. 2013) are just a few of these coatings' standout qualities. They are widely utilized in a variety of industries, including as the petroleum, electro chemical, printing, plastic, space, medical, optical, mining, aerospace, automotive,

nuclear, textile, electronics, computer, paper or food, as protective or ornamental coatings (Agarwala and Agarwala, 2003).

Pure nickel coating, nickel alloy coating, and nickel composite coating are the three different types of EN coatings. The use of a hydrazine bath can produce a pure nickel coating (99%). But due to the hazards associated with hydrazine, it is of little industrial usage (Sudagar et al. 2013).

Pure nickel coating has its uses in the semiconductor applications. Nickel alloy and composite coatings are obtained using alkaline ( $\geq \text{pH } 7$ ) /acidic baths of sodium hypophosphite, sodium borohydride and aminoborane as reducing-agents (Das and Sahoo 2011). The nickel alloy coatings include Ni-P coating and Ni-B coating. Electroless nickel deposits and the addition of additional metal components result in improved mechanical and tribological properties. Electroless nickel poly alloy coatings include Ni-Cu-P (Xu et al. 2014), Ni-W-P (Roy and Sahoo 2013), Ni-P-B (Srinivasan et al. 2010), Ni-W-Cu-P (Balaraju and Rajam 2005), etc. To achieve higher hardness values, self-lubricating, anti-sticking and anti-wear properties additional particles can be co-deposited. They are known as electroless nickel composite coatings and include Ni-P-  $\text{Al}_2\text{O}_3$ , Ni-P-SiC, Ni-P- $\text{TiO}_2$ , Ni-P-PTFE, Ni-P-Diamond etc. (Gadhari and Sahoo 2016; Jiaqiang et al. 2005; Chen et al. 2010; Zhao et al. 2002; Reddy et al. 2000).

Compared to above mentioned nickel alloy and poly alloy coatings, using simultaneous electroless deposition, nickel boron titania (Ni-B- $\text{TiO}_2$ ) composite coatings were effectively applied to mild steel (St-37). Ultrasonic irradiation was used to evenly distribute  $\text{TiO}_2$  particles within a solution. Scanner electron microscopy (SEM), Energy Dispersive X-Ray Analysis (EDX), and X-ray diffraction (XRD) were used to characterize the surface morphology, particle size, elemental composition, and phase analysis of the coatings. Tribo testing (POD) has been incorporated to know the wear and relation between different parameter like load, speed, nano particle percentage and sliding distances. A detailed discussion of the properties of autocatalytically deposited Ni-B- $\text{TiO}_2$  coating has been done subsequently in this chapter.

## **1.6 EFFECT OF PROCESS PARAMETERS ON ELECTROLESS NICKEL-BORON COMPOSITE COATING**

We all know that the electroless coating is an autocatalytic method that widely used. The fundamental constituent of the electroless coating bath are the suitable origin of metallic ions,



an appropriate complexing agent, an acceptable reducing agent, an appropriate complexing agent, and a potentially effective stabilizer. When the substrate with an excessive active surface is submerged in the electroless coating bath, it often generates a potential. Here both positive (+) and negative (-) ions can move in the direction of the substrate material's surface. The transported ions release their energy at the substrate surface, enabling them to adhere to the substrate's surface and create a layer of coating.

The process variables for electroless nickel boron coating are crucial. Every single process variable is important in context of the deposition of Electroless Nickel Coating (EN) coating. The usual electroless bath is made up of an aqueous-solution containing metal-ions, complexing agents, reducing-agents, and stabilizers that operate within a range of pH, temperature, and metal ion concentration. The features of coated components, the rate of deposition, and the structural behavior of deposits are all significantly influenced by the composition and circumstances of the plating bath, including the type and concentrations of the reducing-agent and stabilizer, the used pH, and bath-temperature, etc. Each process variable influences the process response variable and plays a distinct role in the process. Although stabilizer content leads the development of amorphous phase, the stabilizer content has an adverse relationship with the nickel recovery efficiency and directly varied to bath-temperature. Amount of stabilizer has little bearing on coating efficiency. Based on the findings, it was found that when the stabilizer quantity and bath temperature were kept at roughly 25g/l and 85<sup>0</sup>C, a balance between the deposition and decomposition was obtained. In such a coating setting, the coating effectiveness and adhesion both significantly improve. According to research on how different process variables, such as the metal source, the reducing-agent, and the temperature, affect the amount of metal that is deposited per unit area, all of the individual effects are very significant, and the amount of metal deposited increases as the reducing-agent's concentration rises up to a certain point before it starts to decrease. Additionally, it was found that regulating the coating geometry of EN deposition was significantly influenced by the immersion of the nickel-solution and the implementation of the bath temperature with the concentration of reducing agent as well of nickel solution [Sahoo 2008]. Temperature has a substantial impact on deposition as well, and deposition is maximized with the lowering of bath loading [Oraon et al. 2006; Apachitei et al. 1998].

#### **1.6.1 Effect of reducing agent:**

The electroless Nickel Boron(Ni-B) coating method can use a variety of reducing-agents

[Delaunoi set al 2000]. However, the most frequently mentioned reducing-agents for electroless Ni-B coatings are DMAB (dimethylamineborane) and sodium borohydride ( $\text{NaBH}_4$ ).

Depending on the reducing-agent utilized, which is described in Table 1.3, two types of baths—acidic and alkaline ( $\geq \text{pH } 7$ ) baths have often been taken for depositing Ni-B alloy:

**Table 1.3** Different reducing agent for different electroless nickel (EN) plating

Deposition Type	Reducing-agent	Conclusion
Nickel Phosphorus	$\text{NaH}_2\text{PO}_2$	Alkaline( $\geq \text{pH } 7$ ) /acidic bath(3 to 17% P)
Nickel Boron	$\text{NaBH}_4$	Alkaline( $\geq \text{pH } 7$ ) /acidic bath
	DMAB	Alkaline( $\geq \text{pH } 7$ ) bath(0.6 to 11% B)
Only Nickel	$\text{NH}_2\text{NH}_2$	Alkaline( $\geq \text{pH } 7$ ) bath

**(i) DMAB or dimethylamineborane ( $\text{C}_2\text{H}_7\text{BN}$ ):**

DMAB or Dimethylamineborane( $\text{C}_2\text{H}_7\text{BN}$ ) has recently emerged as an appealing reducing-agent for the Ni-B electroless coating bath. It has a distinct amine scent and is a firm, white granule. Its bulk density is between 300 and 350 g/l, and its flash point is 65 °C. DMAB is resolvable in Water ( $\text{H}_2\text{O}$ ), methanol ( $\text{CH}_3\text{OH}$ ) and toluene ( $\text{C}_6\text{H}_5\text{CH}_3$ ) but insoluble in Hexane( $\text{C}_6\text{H}_{14}$ ). DMAB is also used to deposit copper on to electroless nickel(Ni), palladium(Pd) activated plastic, copper metal and many more activated surfaces.

A few of the many advantages that DMAB coating baths offer are their maximum bath-stability, very less working temperatures, better corrosion-resistance, lesser electrical-resistance, and increased quality deposition. Despite its positive effects, it is dangerous and must be handled with the appropriate care [Delaunoi et al. 2000].

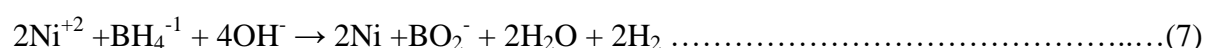
**(ii) Sodium borohydride ( $\text{NaBH}_4$ ):**

Borohydride is a desirable reducing agent for electroless nickel coatings due to its potent reducing activity. When compared to sodium hypophosphite and as per the review made by

Shakoor et al. (2016), sodium borohydride (NaBH<sub>4</sub>) has higher reduction efficiency. The effectiveness Due to its innate capacity to supply more electrons (up to 8electrons) at the time of metal reduction method of same type of reaction as sodium hypophosphite (2 electrons), sodium borohydride(NaBH<sub>4</sub>) is preferred. Additionally, borohydride coating baths are less expensive than DMAB.

The sole negative is that when nickel ions are present in the coating solution, borohydride ions can quickly hydrolyze when exposed to neutral or acidic media, producing nickel boride. To prevent the coating bath from immediately decomposing and to prevent incurring any further costs, this calls for a precise control of pH. A tight control of the coating-bath's pH ranges from 12 and 14 assures the repression of nickel boride production and ensures that nickel will be deposited on the substrate-surface. Because of this, borohydride reducing-agents are frequently utilized in alkaline ( $\geq$ pH 7) medium [Kaya and Demirkol 2009].

In comparison to electroless coatings reduced using other boron compounds or sodium hypophosphite, it is claimed that coatings created with sodium borohydride exhibit improved characteristics. The main advantages of borohydride reduced electroless nickel coatings are their increased wear resistance and high hardness in the synthesized form [Delaunois et al 2000]. The following chemical-reaction equations can be used to depict the electroless Nickel Boron (Ni-B) coating-synthesis reactions.



While reaction (8) makes sure that the formed coatings contain boron, reaction (7) is thought to be responsible for the reduction of Ni ions [Delaunois et al. 2000].

### **1.6.2 Effect of complexing agent:**

The major goals of adding complexing agents to the electroless coating baths are abridged here:

1. It impedes the quick depletion of solution's pH.
2. It prevents the precipitation of coating bath's ingredients like nickel salts.

3. To reduce the quantity of free nickel ions in the coating-bath, promote the creation of metastable complex compounds.

It has also been noted that the complexing agent significantly affects the reaction process and the speed at which coatings develop. Typically, the rate of coating development first increases with increasing amounts of complexing agent and then begins to decline [Shakoor et al. 2014].

A ligand known as a complexing agent interacts to a metal ion to create a complex. There is a lot of use of complexing agents having more than one atom capable of attaching to the main metal atom in a complex in analytical chemistry and industrial chemistry. A poly dentate ligand or chelating agent is the term used to describe such a complexing agent. Three key tasks were discovered for complexing agents in electroless nickel plating baths: (i) lessen the amount of nickel ions that are free. (ii) Exercise a buffering activity to stop the precipitation of nickel phosphite and basic nickel-salts. (iii) Use a buffering technique. The correlation between ligand concentration and plating rate has been researched extensively. The plating rate reaches its maximum as the ligand concentration rises. The plating rate declines as ligand concentration is raised above the point at which the highest rate occurs. The relationship between plating rate and ligand concentration shows that the reaction is sped up by the ligand's low adsorption at the catalytic-surface at small concentrations. Higher concentrations cause the ligand to adsorb heavily on the surface, poisoning the reaction. The rate-increasing section of the curve may be explained more credibly by the complexing agents' buffering effects. When the nickel-ions are still in partial chelating or complexation or when there are still solvated sites on them, maximum rates happen. It must be kept in mind that nickel ions that have partially complexes still have some of the characteristics of free, solvated-nickel ions. Therefore, the primary role of the different ligands is buffering up to the concentrations where the highest plating rates occur.

### **1.6.3 Effect of temperature:**

Another crucial element for the characteristics of Nickel Boron (Ni-B) electroless coatings is temperature. It was discovered that the temperature affects both the complexing and reduction agents in the Ni-P electroless process. The coating in the sodium hydroxide baths is significantly impacted by temperature. It is well known that plating doesn't happen much, if at all, below 60 °C. The rate of plating rises exponentially as temperature rises. Operating temperatures for acid hypophosphite plating solutions range from 80° to 90°. If the

temperature is allowed to rise considerably over 90°C, there is a greater chance of solution breakdown or perhaps solution plate out. When the plating bath's temperature is raised above its typical operating range while maintaining all other conditions, the boron concentration of deposits decreases. In case of electroless Nickel Boron (Ni-B), the operating temperature is generally kept at  $85^{\circ} \pm 3^{\circ}$ , above that value the bath-temperature likely to be unstable [Agarwala and Agarwala 2003].

#### **1.6.4 Effect of pH value:**

Saito et al. (1998), investigated how Ni-B and Co-B coatings responded to pH changes. The amount of deposition per minute and amount of boron of the alloys are measured as the function of solution pH. According to reports, no sooner the solution's pH increases oxidation of Dimethylamineborane ( $C_2H_7BN$ ) and the amount of deposition per minute of electroless Nickel Boron (Ni-B) and Cobalt Boron (Co-B) coatings both increase. However, the boron concentration of Nickel Boron (Ni-B) coatings is barely impacted by the pH of the solution. In this instance, it is found that the contented boron and amount of Ni-B deposition are inversely correlated. As per the review by Narayana et al. 2004 on Ni-Co-B coatings, at beginning the bath's pH uplift the coating rate as late as it reaches the saturation ( $300 \text{ mg/cm}^2/\text{hr.}$ ) at around pH eight, and if further we change increase the pH value it rapidly decreases the coating rate.

The amount of  $H^+$  ions rises when the metal is formed from reduced nickel ions. This has the direct implication that pH will decrease as electroless deposition advances. All electroless baths must therefore include a buffer and continuously dose diluted alkali to supply  $OH^-$  ions throughout operation. Table 1.4 illustrates how pH affects solution and deposition. The inherent stress in the EN deposition is significantly influenced by pH value, aged solution, and their compounding effects [Chen et al. 2003].

The production of brilliant and adhering deposits was shown to increase coating thickness as the bath pH rose from 8 to 10. However, the bath decomposes and the coating thickness significantly reduces at higher pH levels ( $pH > 10$ ) [Aal et al. 2008].

**Table 1.4** Change of pH value on solution and deposition

Change of pH	Effect on bath solution	Effect on coating deposit
Increasing pH	a) Decreases phosphite (P) solubility and increases deposition rate b) Stability decreased as resultant plate out	a) As the phosphite (P) content decreases then stress shifted to tensile direction b) Weaker adhesion in steel
Decreasing pH	a) Deposition rate decreases and it improves solubility of phosphite (P).	a) As the phosphite (P) content increases then the stress shifted to compressive direction. b) Strong adhesion in steel.

**1.6.5 Effect of time:**

As coating duration increases, the coating rate also rises. The coating will be thicker as the longer time is provided for coating. However, the rate of rise in thickness is not maintaining straight line over the course of plating; it saturates after a while [Krishnaveni et al. 2005] and gets smaller as time goes on. This behavior may be caused by the oxidation products that occur in electroless plating baths and the gradual decrease in the concentration of DMAB [Hamid et al. 2010].

**1.6.6 Effect of surfactant:**

In order to improve wetting action and reduce the surface-tension of the coating-bath solution, surfactants are frequently used. A coating bath's effective usage of surfactants makes it easier for coating material to spread smoothly and lowers the forces between the molecules phase of the concerned solution and a solid's surface. The correct amount of surfactant is usually added to the electroless nickel bath to increase coating deposition rate [Sahoo and Das, 2011]. Although surfactants have been fairly reported to be used in baths for coating Ni-P [Elansazhian et al. 2008], their usage in baths for coating electroless Nickel-Boron (Ni-B) is not very common [Kanta et al. 2009].

#### **1.6.7 Effect of stabilizers:**

Despite the application of the effective complexing agent, the bath solution exhibits inconsistent and produces the precipitation of metal. Some compounds, referred to as stabilizers, are mixed with the plating bath solution just to avoid or reduce the unwanted metal powder precipitation [Krishnaveni et al. 2002]. According to Delaunois et al. (2002), the use of suitable stabilizers is crucial for a regulated reduction-reaction in the electroless Nickel Boron (Ni-B) bath. A careful selection of the stabilizers in the electroless coating solution can be used to regulate the reduction reaction, which in turn controls the amount of deposition per minute and guarantees that the plating layer forms on the substrate. The stabilizers prevent nickel reduction on many of the solution's particles by adhering to their surfaces throughout their action. Numerous stabilizers with promising performance are readily available. The choice of stabilizer must be made carefully. According to some accounts, the electroless coating baths can be stabilized rather effectively with mercaptobenzothiazole and lead nitrate. However, the deposition rate for these is weak. In order to achieve good bath stabilization with high deposition rates, thalium compounds such thalium nitrate are appealing stabilizers [Sankara et al. 2004].

#### **1.6.8 Effect of buffering agents:**

The maximum amount of buffer content of the complexing agents and more substances known as buffers which are exist the bath affects how much the pH affects with the production of  $H^+$ . Simply said, a buffer is the material or combination of compounds that, when mixed with a solution, may neutralize both acids and bases without significantly altering the solution's initial pH. The volume of acid ( $H^+$ ) required to modify the pH with the specific volume is a measure of buffer capacity. The buffer performs better when more acid is necessary. An electroless nickel plating bath's practical buffer capacity, PB, can be calculated by by-titrating of standard acid solution and executing pH vs. acid concentration.

#### **1.6.9 Effect of heat treatment:**

The characteristics of a material establish its specific application, and adherence to a desired set of characteristics ensures safe and effective use. Numerous techniques, like heat-treatment (hardening, annealing, normalizing), thermo-mechanical treatments etc., can be used to

increase the mechanical property of bulk materials, like toughness, strength, hardness, wear and scratch resistance etc. Coatings with boron levels over 4 weight percent typically behave amorphously. Heat treatment can cause the deposit to crystallize and develop grains, which has a significant impact on the structure and characteristics of these coatings [Vitry et al. 2012]. Using DMAB as a reducing-agent, Hamid et al. (2010) looked into how Nickel Boron coatings' crystal-structure, micro hardness, amount of deposition and corrosion behavior were affected by the deposition temperature and heat treatment. Their XRD patterns make it abundantly evident that electroless Nickel Boron (Ni-B) coatings coated in between 60°C and 80°C are amorphous when they are first applied and undergo phase-transformation at the time of heat treatment process. It is discovered that the heat treatment procedure can significantly increase micro hardness. They have also reported on how heat treatment affects micro hardness. According to reports, hardness rises as temperature rises. It is thought that the nucleation of crystalline phases like  $\text{Ni}_3\text{B}$  is what caused this increase in hardness.

According to studies on the impact of heat treatment temperature on corrosion behavior, the least amount of corrosion found for Ni-B coatings heat treated at 400 °C (applicable for both copper or steel-coated samples), and an enhancement of roughly 95% times is observed in comparison to substrates. The full nucleation of crystalline  $\text{Ni}_3\text{B}$  into the Ni-B matrix is responsible for the improvement in corrosion behavior. These results suggest that Ni-B coatings establish a protective film on the exterior of the substrate, reducing the substrate's susceptibility to attack by chloride ions. In contrast to the observations made above, heating Ni-B coatings to 250°C has somewhat increased the rate of corrosion compared to both the substrates (steel or copper) and the coatings in their as-deposited form. The partial conversion of amorphous structure to microcrystalline can be used to explain this shift in corrosion behavior [Hamid et al. 2010].

Electroless Nickel Boron(Ni-B)coatings are typically formless in nature when they are first deposited, but with the right thermal treatment, they can become crystalline [Sankara et al. 2004 and Delaunois et al. 2002]. According to reports, when the temperature rises, the amorphous structure becomes crystalline, forming crystalline phases like  $\text{Ni}_2\text{B}$  and  $\text{Ni}_3\text{B}$  in the microstructure [Sankara et al. 2004].

Electroless Nickel Boron (Ni-B) coatings shows an excessive hardness, according to reports [Dervos et al. 2004], the mechanical qualities of an object are significantly impacted by the heat treatment process. After the vacuum heat treatment technique, a notable increase in hardness has been noted. Numerous more study reports [Vitry et al. 2012; Delaunois et al.



2002] have similar studies.

The impact of heat-treatment on the wear as well as hardness of electroless Nickel-Boron (Ni-B) coating on alumina alloys was documented by Delaunious et al. [Delauniois et al. 2002]. At various heat treatment temperatures and soaking durations, they measured the coatings' Knoop hardness. According to reports, the Ni-B-Pb plating, hardness rises as the heat-treatment temperature as well as wetting time increases. This improve in hardness may be attributable to the heat treatment procedure, which converts the amorphous structure into crystalline. Heat treatment temperature ( $^{\circ}\text{C}$ ) vs. Hardness (VPN) is shown in Fig. 1.5 [Delauniois et al. 2002].

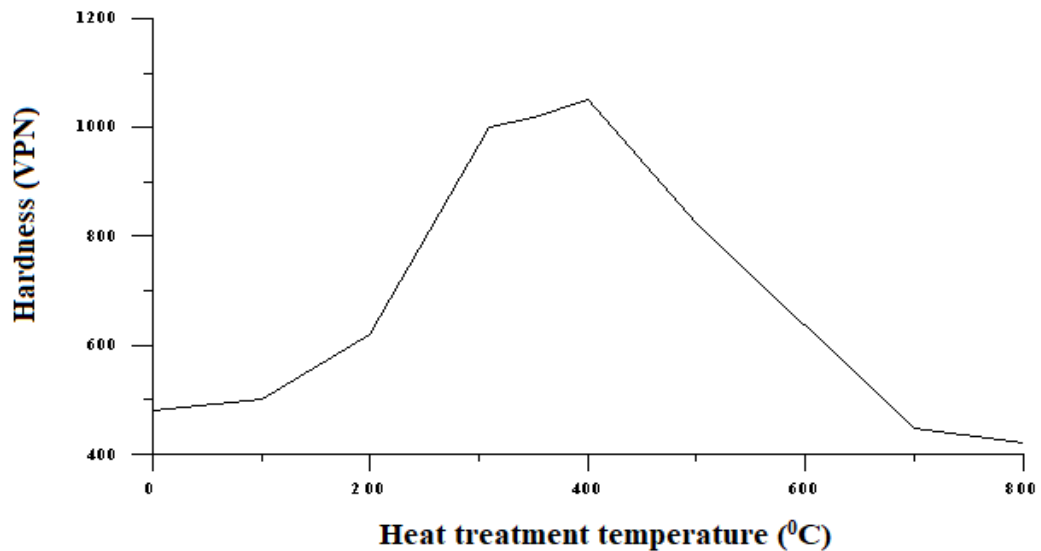


**Fig. 1.5** The hardness of Ni-B coatings is influenced by the temperature of the heat treatment [Delauniois et al. 2002].

## 1.7 LITERATURE REVIEW

Due to their unique features, nickel boron(Ni-B) and nickel phosphorus(Ni-P) electroless nickel coatings have become largely accepted in the engineering field during the past few decades. During this time, vast amount of research has been done on the physio mechanical characteristics of electroless nickel coatings. Corrosion resistance is one of the key qualities

of electroless nickel coatings. To make electroless Ni-P coatings more resistant to corrosion, numerous works have been done. The suggested techniques include ternary alloy formation in presence of a 3rd element like Mg, Zr, Cu etc., duplex-coating or ENIG i.e. nickel immersion-gold surface electroless coating. It is also comprises composite-coatings by adding  $\text{CuSO}_4$ ,  $\text{SrO}_2$ ,  $\text{Al}_2\text{O}_3$ ,  $\text{TiO}_2$  etc. [Song et al. 2008 ; Rabizadeh et al. 2011].

In context of hardness as well as wear-resistance in common, Ni-B is more preferable than Ni-P coating [Sudagar et al. 2013]. Again to improve more and more hardness and wear-resistance  $\text{TiO}_2$ ,  $\text{Al}_2\text{O}_3$ , diamond, BN etc. can be applied in Ni-B coating [Dehghanian 2011, Yu et al. 1993 , Guo et al. 1995, Quo et al. 1997, Shen et al. 2007, Kaya et al. 2008].

Vast study has been made to measure the effect of bath-composition and deposition, heat operation in favor of corrosion characteristics of Ni-B coatings. Alkaline ( $\geq \text{pH } 7$ ) and acidic baths are two different category of baths that suggested for the electroless Nickel Boron (Ni-B) coating deposition process. Sodium borohydride or the amino boranes N-dimethyl amine borane(DMAB) and N-diethylamineborane (DEAB) are utilized as reducing-agents for the deposition. The most effective and popular reducing agent to get the electroless Nickel Boron(Ni-B) coating is sodium borohydride. Borohydrides are easily hydrolyzed in the acidic and neutral pH ranges, and nickel boride is produced when nickel ions are present. Therefore, pH control is required to stop the electroless bath from instantly decomposing. The synthesis of nickelboride is prevented and the deposit primarily made up of fundamental nickel if the pH is kept between 12 and 14. Both acidic and alkaline ( $\geq \text{pH } 7$ ) conditions can be used with nickel baths that use amine boranes as the reducing-agent. Overall, nickel metallic and nickel boride are produced. Amineboranes are good reducing-agents for the electroless deposition on ceramics, plastics, nonmetals and additionally some other metals like Magnesium, Copper, Aluminum etc. Typical table content showed in details by Table. 1.5 [Sudagar et al. 2013].

**Table 1.5** Common electroless nickel coating bath applications, operating circumstances, and component types.

Electroless coating bath	Pure nickel(Ni)	Acid nickel : P or B	Alkaline( $\geq \text{pH}7$ ) nickel: P or B
Hydrogen potential(pH)	10.4 to 10.9	4.5 to 5.5 Medium & high P or B; 6.0 to	8.5 to 14

		6.5 low P or B	
Temperature in degree Celsius(°C)	85 to 90	75 to 95	25 to 95
Rate of Deposition( $\mu$ m per hour)	6 to 12	10 to 25	10 to 15
Metal salts or source	Nickel acetate( $C_4H_6NiO_4$ )	Nickel Chloride( $NiCl_2$ ), ,Nickel Sulphate ( $NiSO_4$ )	Nickel Chloride( $NiCl_2$ ), ,Nickel Sulphate ( $NiSO_4$ )
Bath Reducing- agents	Hydrazine( $NaBH_4$ )	Sodium Borohydride Hydrazine( $NaBH_4$ ), Sodium Hypophosphite( $NaPO_2H_2$ ), DMAB i.e. dimethylamine	Sodium Borohydride Hydrazine( $NaBH_4$ ), Sodium Hypophosphite ( $NaPO_2H_2$ ), DMAB i.e. dimethylamine
Complexing agents	EDTA i.e. Ethylenediamine tetraacetic acid ( $C_{10}H_{16}N_2O_8$ ), glycolic acid.	Succinic acid( $C_4H_6O_4$ ), Citric acid, lactic acid , glycolic, Sodium citrate( $Na_3C_6H_5O_7$ ) .	Succinic acid( $C_4H_6O_4$ ), Citric acid, lactic acid , glycolic, Sodium citrate( $Na_3C_6H_5O_7$ ) .
Stabilizer		Thiourea( $CH_4N_2S$ ), lead(Pb), acetate ( $CH_3COOH$ ), metal salts, thioorganic	Lead, Tin, Arsenic, Molybdenum, Cadmium or Thallium ions
pH Controllers		Sodium hydroxide( $NaOH$ ), sulfuric acid( $H_2SO_4$ ).	Sodium hydroxide ( $NaOH$ ), sulfuric acid( $H_2SO_4$ ).

When compared to sodium borohydride in reference of boron compounds or sodium-hypophosphite with respect to reduced-deposition sodium borohydride is superior here it has significantly higher wear resistance and hardness in electroless nickel coating.

By adjusting the coating bath parameters, including bath temperature and pH, as well as the coating parameters, electroless Nickel Boron coating deposition rate can be adjusted. The rate at which electroless Nickel Boron coating is deposited enhance with increasing sodium borohydride content. As buffer content, specifically NaOH concentration, increases, so does the amount of plating. The rate of deposition increases initially and then declines with an increase in the complexing agent (Ethylenediamine). The deposition finally rises to 85<sup>0</sup>C with an increase in bath temperature before once more beginning to fall. The management of the bath composition is one of the challenges in reduction processes or chemical plating. Stabilizers are required to manage the reduction process. They manage the reduction reaction such that just the substrate that needs to be plated is affected by the deposition, which happens at a predictable rate(Delaunois and Lienard, 2002). They prevent the decrease of nickel on their surface by adhering to numerous colloidal particles in the solution. Then, many stabilizers can be utilized effectively. Thallium nitrate is the first one. However, due to its toxicity and environmental issues, lead tungstate can be used in its place without any issues with bath stability or deposition rate. Along with thallium nitrate, some stabilizers may added simultaneously in the Ni-B coating, which can result in the production of a ternary alloy like Ni-B-Tl. They might also improve the deposit's appearance (Baudrand 1994). Stabilizer has a considerable impact on the pace of deposition. Thallium ions improve the reduction efficiency of borohydride and stabilize the plating bath in addition to being a superior reducing-agent than lead nitrate, which results in a slower plating rate.

It has been discovered that the electroless Ni-B coatings' weak or average corrosion-resistance is one of their biggest disadvantage. For this reason duplex-coating like (Ni-P with Ni-B) has been proposed by several researchers [Narayanan et al. 2003, Zhang et al. 2008, Kanta et al. 2009, Vitry et al. 2012].They have implemented nitridingmethod[Vitry et al. 2012], different thermo-chemical methods like Taiwan Carbon Nanotube Technology (TCNT) and Triazacyclononanetriacetate(TCTA), to enhance the corrosion property of the said coatings. But these are not suitable as per the experiment set up a well as cost.Nowdays, TiO<sub>2</sub>is one of the best alternatives for coating composites among the scientists for its variety of industrial uses specially its improved hardness and corrosion resistance in the coatings.

### **1.7.1 Tribological studies of electroless nickel boron tinania (Ni-B-TiO<sub>2</sub>) coating:**

It is most significance that the performance of a material in respect of engineering achievement and its existence directly depends upon the surface characteristics of the said materials in the wide range of industrial application and the improvement of the material surfaces depends upon the coating characteristics.

Due to the fact that this coating was unable to provide the needed surface properties, several nano particles were added to it in order to increase its ability to possess the desired physical, chemical, and mechanical capabilities [Kanani 2004]. According to Brooks et al. (2008), the stronger and harder nano composite covering is a result of their higher grain boundary densities. Electroless Nickel-Boron (Ni-B) coatings were strengthened using ultrasonically sonicated nanoTiO<sub>2</sub> particles. Maseoud et al. (2021), showed the improvement of different types of wear properties likely abrasive or impact wear of Ni-B-TiO<sub>2</sub> composite-coating and also showed its utility that how the nano particles improves the wear resistivity of both the combined hammering effect of impact wear as well as abrasive wear by reducing material losses. Wang et al. 2012, have also examined the tribo-mechanical properties of Ni-B-TiO<sub>2</sub>.

Table 1.6 [Maseoud et al. 2021] displays the result of heat-treatment with respect to mechanical characteristics (micro-hardness, elastic modulus etc.), roughness and particle size of the substrate and the examined coatings. Additionally, the impact of TiO<sub>2</sub> nanoparticles on the properties of pure Ni-B plating is taken into account. To enhance the micro-hardness of AISI P20 steel from 5300±300 MPa to 9000±800 MPa, heat-treatment is mostly desired, though the elastic modulus of that steel almost remains same. As per as coating is considered, it is apparent that they display a significant micro hardness in both their annealed and non-annealed states. In the meantime, the coating heat-treatment leads the growth of the grain size. The diffusion of tiny Ni grains during the annealing process is blamed for the latter. When it comes to grains that are nanoscale, this phenomena occurs. The coating's roughness is unaffected by the heat treatment process. Maseoud et al. (2021) found that the micro-hardness decreases from 13600 MPa to 12600 MPa as the TiO<sub>2</sub> soft nanoparticles impeded into the Ni-B composite coating with annealed-condition, irrespective of the reduction of Ni grain size. So, as to introducing of TiO<sub>2</sub> in Ni-B coating helps to refinement of nickel grain-size that is not consistent in respect to the Hall-Patch-effect [ZH et al. 2012]. The same results obtain by Sun et al. 2015 when different content of graphite impeded to Ni-Al<sub>2</sub>O<sub>3</sub> composite. Till, implementing the TiO<sub>2</sub> nanoparticles

**Table 1.6** Micro hardness, elastic modulus, grain size and roughness

Material	Micro hardness (GPa)	Elastic modulus (GPa)	Grain size (nm)	Roughness Ra ( $\mu\text{m}$ )
AISI P20 as - received	$5.3 \pm 0.3$	$295 \pm 17$		
AISI P20 after heat treatment	$9 \pm 0.8$	$287 \pm 21$		$0.073 \pm 0.005$
Ni-B (non-annealed)	$12.5 \pm 0.3$	$246 \pm 4$	$4.8 \pm 1$	$0.11 \pm 0.03$
Ni- B (annealed)	$13.6 \pm 1$	$262 \pm 5$	$16 \pm 2$	$0.11 \pm 0.03$
Ni-B-TiO <sub>2</sub> sol (non-annealed)	$11 \pm 0.4$	$257 \pm 10$	$5 \pm 1$	$0.12 \pm 0.03$
Ni-B-TiO <sub>2</sub> sol (annealed)	$12.6 \pm 0.5$	$264 \pm 6$	$13 \pm 1$	$0.12 \pm 0.03$
* After mechanical polishing				

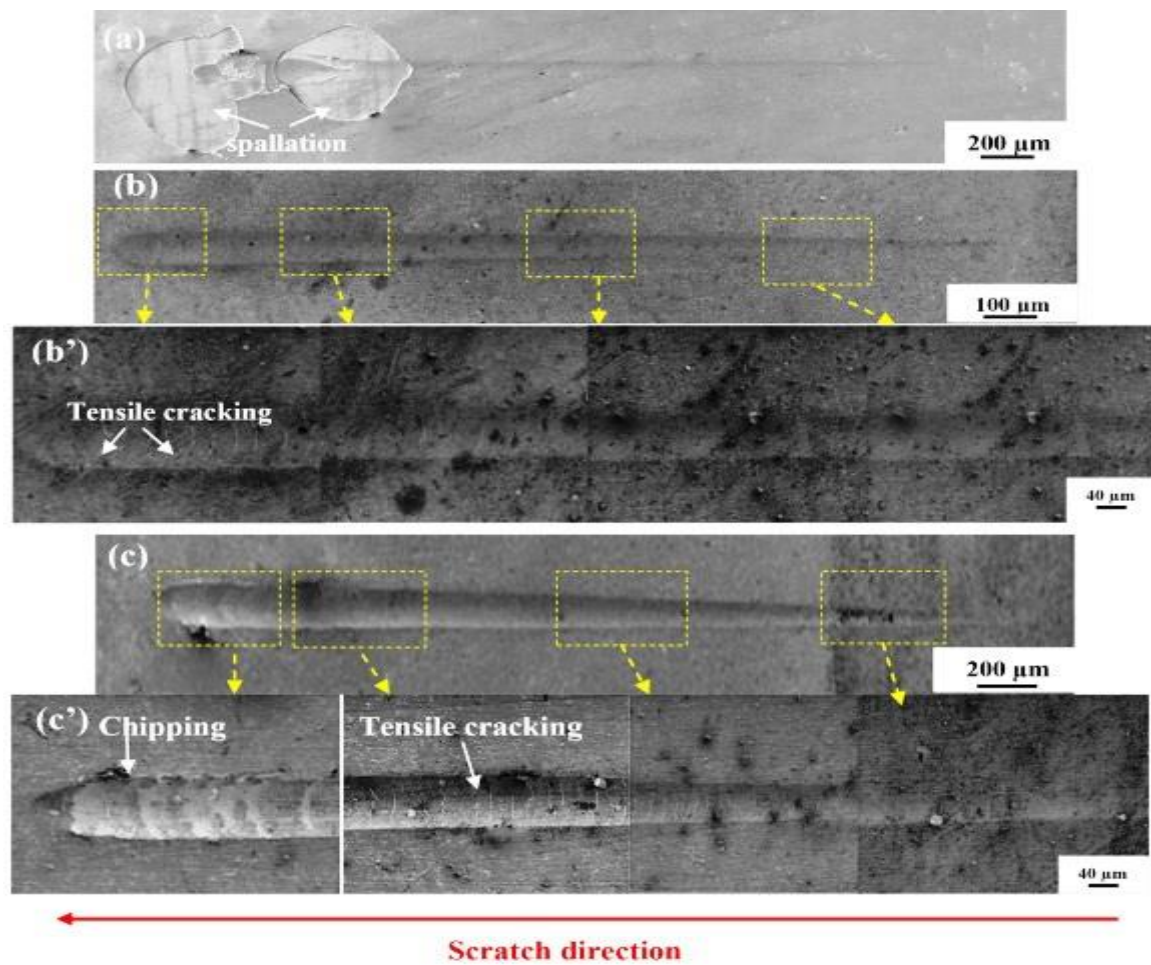


**Fig. 1.6** Scratches traces: (a) Ni-B coating (b) Ni-B-TiO<sub>2</sub> composite coating @ indenter tip radius 200mm. (c) scratch test: @ indenter tip radius 100mm in progressive load (Masseoud et al. 2021).

enhanced the elastic-modulus as well as surface-roughness of Ni-B coating. More interestingly coating thickness (12 $\mu$ m) not affected by the heat treatment or the TiO<sub>2</sub> nano particles. Here, increasing load-scratch test by the help of different indenters (tip radii 100  $\mu$ m and 200  $\mu$ m) is applied to measure the adhesion-strength of nickel boron coating in presence of TiO<sub>2</sub> nanoparticles. Two different scratch test conducted in pure Ni-B as well as Ni-B- TiO<sub>2</sub> sol nano composite coating by the scratching with the 200 $\mu$ m tip radius indenter that revealed the report as shown in the Fig. 1.6 [Masseoud et al. 2021]. It signifies that how adding of TiO<sub>2</sub> nanoparticles enhance the adherence-performance of Ni-B matrix.

### **1.7.2 Micro structural, thermal and chemical studies:**

The samples were obtained up to 500<sup>0</sup>C, and XRD phase inspection [Fig.1.7] shown that they were a mingleof phases (anatase and brookite). Being a mono phase, rutile was found to be present in the solution at 850<sup>0</sup>C and above. The processing of TiO<sub>2</sub>, samples had an impact on the TGA/DTA curves [Fig. 1.8]. The amorphous TiO<sub>2</sub> particles increased in size to 0.7  $\mu$ m after approx. 10 minutes of chemical decomposition in aqueous solution at room-temperature. Chhor et al. (1992) looked into how the experimental process affected the micro-structure of TiO<sub>2</sub>. TiO<sub>2</sub>dusts were obtained from Ti (Iv-isopropoxidethrough 3 separate methods, (a) thermal decomposition of titaniumalkoxide (C<sub>12</sub>H<sub>28</sub>O<sub>4</sub>Ti) in vapourphase, (b) decomposition of titaniumisopropoxide in supercritical CH<sub>3</sub>OH(ethanol) and (c) standard method of hydrolysis of Ti(IV)-iso-propoxide dissolved in ethanol. The conditions of TiO<sub>2</sub>, fiber formation by hydrolysis and poly-condensation of Ti(IV) iso-propoxidewere studied by Kamiya et al. (2022). The sol-gel approach requires sincere regulation of the conditions for the formation of primarily chain-like or linear metaloxanepolymers in solutions through the chemical decomposition in aqueous solution and poly-condensation processes. This indicates that a key variable in the synthesis of TiO<sub>2</sub>, fibers is the primary molecular ratio of Tialkoxide to H<sub>2</sub>O. Researchers looked on the relationship between TiO<sub>2</sub>composition and the solgel synthesis specifications (hydrolysis-catalyst, pH and applied temperature below the melting point) [Lopez et al. 1992]. Immediately following the heat treatment of the TiO<sub>2</sub> precursor, extremely acidic and alkaline-catalysts encouraged the production of rutile. It was discovered that the pH of the reaction had no effect on the particles' size or form. During the synthesis of TiO<sub>2</sub>along with oxalic-acid, an exception was noticed. The impact of H<sup>+</sup> ions in production of titaniumoxopolymers was investigated by Kallala et al. 2011, the authors measured the ultimate shape of the polymers in gels created under different reaction

postulates using the hydrolysis-ratio, since it determines the potential working of monomers, the obstruction ratio, which selects the relative measures of various reactions, and the monomer-concentration, which determines the maximum size that the polymers can reach before intergrowth. It was proposed that development occurred in two stages, with a little large polymers forming initially before being engulfed by other monomers to become denser. Terabe et al. 1994 looked into how hydrochloric (HCl) and water(H<sub>2</sub>O)acid affected the shape and crystallization behavior of TiO<sub>2</sub> a sol gel prepared precursor. Small angle X-ray scattering (SAXS) was used to analyses particle-aggregation in the time of the early freezing phase of the solgel synthesis of TiO<sub>2</sub> [Kamiyama et al. 1994].

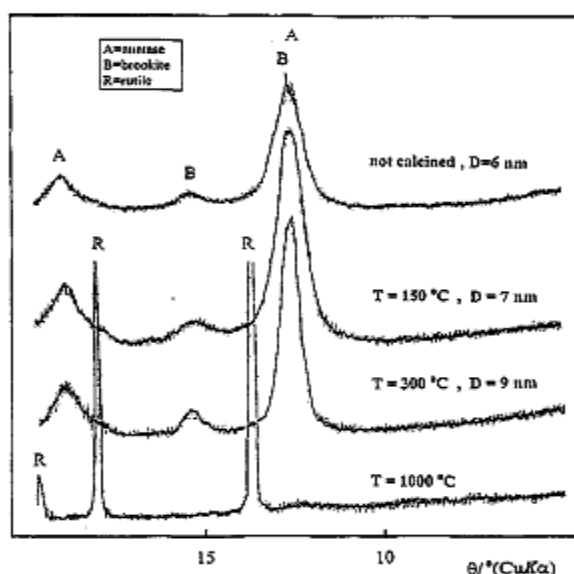


**Fig. 1.7** Characteristic part of the XRD power pattern of the TiO<sub>2</sub> sample and its thermal deposition products A<sub>1</sub> (150°C), A<sub>2</sub> (300°C), A<sub>5</sub> (1000°C). (Kamaya et al. 2022)

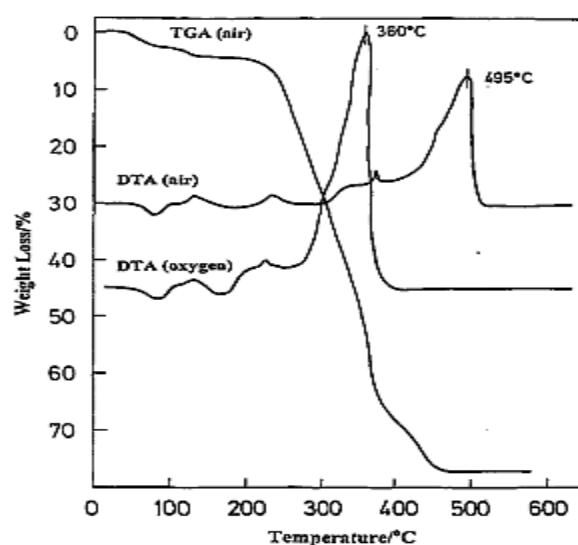


**Fig. 1.8** TGA and differential thermal analysis i.e. DTA on TiO<sub>2</sub> (stabilized with polyethylene glycol or PEG) @ heat rate 10<sup>0</sup>C per minute (Kamaya et al. 2022).



### 1.7.3 Deposit hardness:

One of the important tribological characteristics of ENB coating technology is deposit hardness. The film composition (% B), temperature and duration of the heat treatment are factors that influence hardness. The ENB deposits when plated typically have micro-hardness values between 600 and 700 VHN. It was discovered that the outcome of thermo-mechanical treatment varies depending on the coated samples. In contrast to medium and thick coated steel, thin coated steel experiences a substantial change in surface morphology during heat treatment and its hardness gradient is much smaller than that of thick and medium coated steel. Fig. 1.9 [Harun GÜL 2023] shows thickness and hardness values derived from different samples like Nickel, Nickel-Boron (1.85% Boron) and Nickel Samarium films.

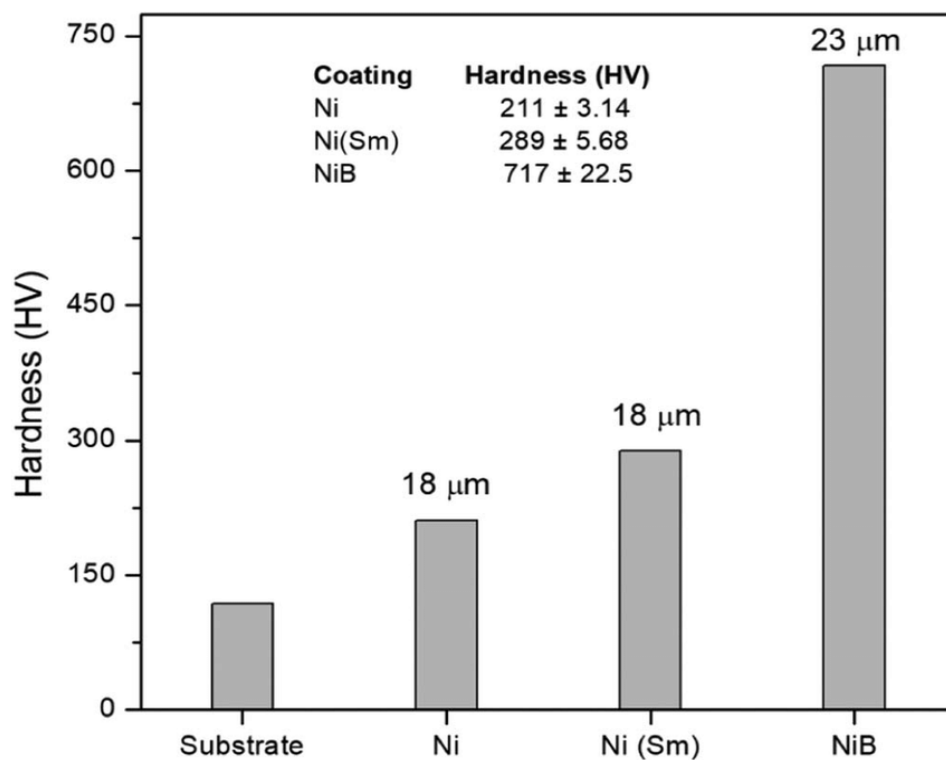


**Fig. 1.9** Comparison of hardness as well as thickness values for different coatings like Ni, Ni-B (1.84% Boron) and Ni(Sm) films (GÜL, 2023).

### 1.7.4 Summary of literature review:

This literature review reflects in details about the coating process and its effectiveness in context of bath composition to micro structural analysis aiming to improve the surface

properties. In order we can sum up as follows:

- (i) A comparison analysis is done in between different coatings like Ni-B vs Ni-P coatings which shows that in context of hardness as well as wear-resistance in common, Ni-B is more preferable than Ni-P coating. Again to improve more and more hardness and wear-resistance  $\text{TiO}_2$ ,  $\text{Al}_2\text{O}_3$ , diamond, BN etc. can be incorporated in Ni-B coating.
- (ii) An extensive discussion is made how the deposition can be improved. For example, by adjusting the coating bath parameters, including bath temperature and pH, as well as the coating parameters, electroless Nickel Boron coating deposition rate can be improved.
- (iii) The review emphasizes how the corrosion resistance can be improved. It has been discovered that the electroless Ni-B coatings' weak or average corrosion-resistance is one of their biggest disadvantage. For this reason duplex-coating like (Ni-P with Ni-B) has been proposed by several researchers.
- (iv) The review tried to focus on the cost effectiveness of the coatings as well as the improvement of the mechanical properties. For example, we can select different thermo-chemical methods like Taiwan Carbon Nanotube Technology (TCNT) and Triazacyclononanetriacetate (TCTA), to enhance the corrosion property of the said coatings. But these are not suitable as per the experiment set up as well as cost. Now days,  $\text{TiO}_2$  inspired among the scientists for its variety of industrial uses specially its improved hardness and corrosion resistance in the coatings.
- (v) The review covered the morphological areas of the coatings for the desired physical, chemical, thermal and mechanical capabilities in context of improvement of mechanical properties like micro hardness, elastic modulus along with the views of grain size and surface roughness.

## **1.8 PRESENT WORK**

It is evident from the thorough analysis of the literature that electroless nickel-boron coating has several uses and that extensive research has been done to enhance its characteristics. The majority of research has been done to increase the deposits' hardness while lowering friction and wear. Additionally, the deposition mechanism has been looked into and it was discovered that the coating had strong adhesion and corrosion resistance qualities.

Implementing the  $\text{TiO}_2$  nanoparticles enhanced the elastic-modulus as well as surface-roughness of Ni-B coating but at the same time micro-hardness decreases  $\text{TiO}_2$  in Ni-B coating helps to refinement of nickel grain-size [Masseoud et al. 2021]. In this present study it is explained later that how Ni-B- $\text{TiO}_2$  coating improved mechanical properties with respect to Ni-B coating considering scratch and corrosion-resistance. The strong nano  $\text{TiO}_2$  particles enhance the scratch-resistance of the Nickel-Boron- $\text{TiO}_2$  coatings. The corrosion behavior was also greatly enhanced by the use of nano particles. The reduction of porosities in presence of  $\text{TiO}_2$  is observed in Cdl characteristics. The object used for SEM morphology. By adjusting the tribo testing parameters determined by the Taguchi method, the current work also makes an effort to analyze the variation in wear and friction coefficient of electroless Nickel-Boron (Ni-B) - $\text{TiO}_2$  coating under dry sliding conditions. The tribological performance of Ni-B coating and Ni-B- $\text{TiO}_2$  composite has been compared.

## **1.9 PRESENT THESIS**

There are four chapters in the current thesis. The first chapter provides a general overview of electroless nickel coatings, their applications and consequent Literature Review i.e. survey of relevant academic literature on electroless nickel-boron coating. The details of the experimental procedure are provided in the second chapter. In chapter three, a thorough examination of the results was completed. The crucial findings that have been drawn from the current study and the work's future prospects are finally included in the four chapters.

---

## **EXPERIMENTAL METHODS**

*A summary of the coating process, materials and equipment used, selection of process parameters, response variables, design of experiment (DOE), analysis of variance for the experiments are discussed in this chapter.*

### **2.1 INTRODUCTION**

From the extensive literature review it is understood that electroless Ni-B-TiO<sub>2</sub> coating deposition can be improved by different coating bath parameters which is directly related to the experimental methods and procedure. The method for depositing an electroless Nickel Boron Titania (Ni-B-TiO<sub>2</sub>) coating and the sequence of experiments that were carried out to get the study's conclusions are described in this chapter. Deposition is carried out on mild steel specimens as per the DOE by Taguchi method. Wear and friction tests are carried out by tribo tester. Scratch and corrosion tests are also done as per the procedure. The details of the whole experimentation process have been discussed elaborately. Following steps has been taken out to fulfill the requirements (Fig. 2.1):

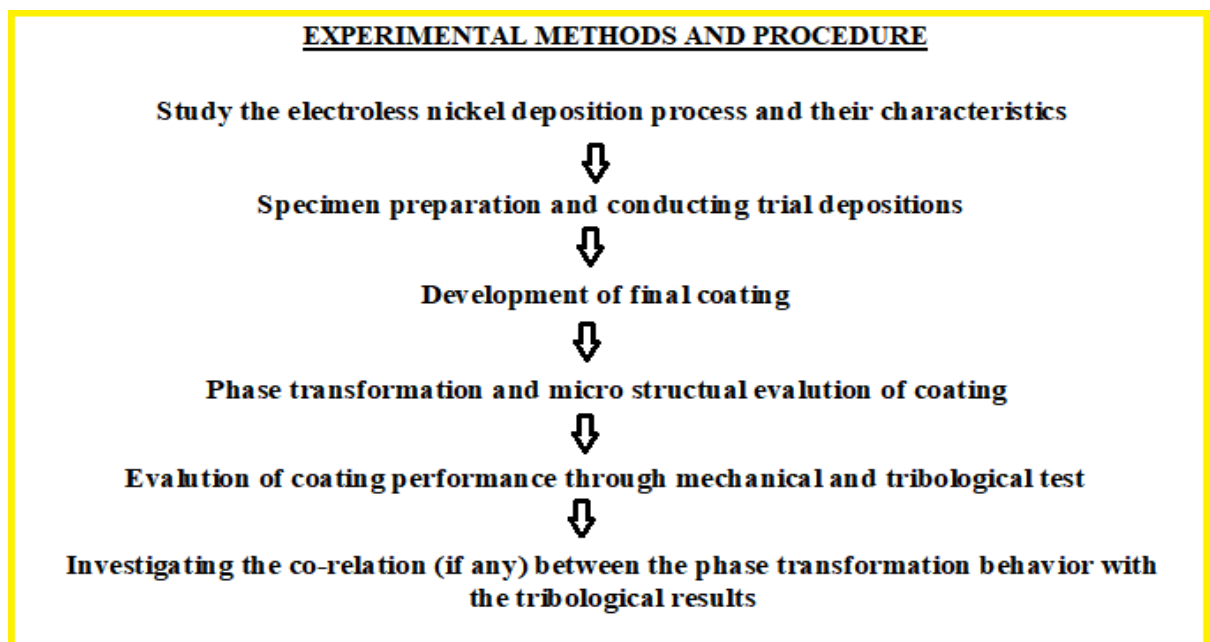


**Fig. 2.1** Flow chart: experimental methods and procedure

## **2.2 DEPOSITION OF ELECTROLESS NICKEL BORON TITANIA (Ni-B-TiO<sub>2</sub>) COATING**

### **2.2.1 Preparation of substrate:**

The specimen was metallurgical formed prior to be deposited. Mild steel (AISI-1040) samples of dimension Ø6 mm x 30mm are taken as the specimen to be deposited in the electroless Ni-B-TiO<sub>2</sub> coating. Turning facing parting and grinding are the machining operations that have been used in this experiment to get the substrate of desired dimensions and surface finish. Turning operation is used to obtain the desired diameter of the substrate or rather the pin on which coating is deposited to adjust with the mechanical system of the pin-on-disc tribo tester. Similarly to obtain the desired length of the mild steel specimen, facing and finally parting operations are employed. By rubbing and cleaning, the specimens are made free of debris and rusts. The samples are subsequently put through a method of surface-grinding. To get uniformly smooth specimens with the same level of surface-roughness, the samples were gleamed with emery sheets of grades (800, 1400, and 1800). The specimens were then ultrasonically cleaned, dipped into the acid and dried. Again it is dipped into the palladium chloride bicker (heated with 50<sup>0</sup>C) for 10 seconds for itching as well as to react in deposition operation.

### **2.2.2 Preparation of bath:**

The bath configuration of different ingredient is stated in the following Table 2.1. In a washed beaker, 250 ml of the bath solution were created. The experiments were carried out by the magnetic stirrer (IKA, India) fitted with small temperature controller. The complexing agent employed was ethylenediamine (C<sub>2</sub>H<sub>8</sub>N<sub>2</sub>). The main purpose of the complexing agents is to restraint and stops the solution's required pH (12–14) from dropping sharply. Additionally, complexing agents aid in preventing the precipitation nickel metal in the bath [Agarwala and Agarwala 2003]. The origin of the Ni<sup>+2</sup> ions in the solution was nickel chloride hexahydrate (H<sub>12</sub>Cl<sub>2</sub>NiO<sub>6</sub>). Before using the TiO<sub>2</sub> nano powder it was ultrasonicated in distilled water for 30 minutes with the frequency 60 Hz and then it is poured into the bath just after 5 minute of introduction of the specimen. The Ni<sup>+2</sup> ions are reduced using free electrons from sodium borohydride (NaBH<sub>4</sub>). The experiment is carried out by 1 hr30 minutes and the bath temperature of 85<sup>0</sup>C to 88<sup>0</sup>C was kept constant.

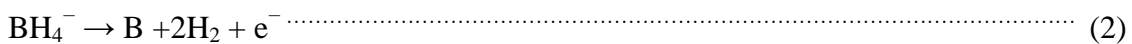
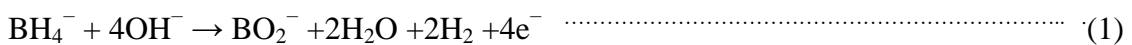
**Table 2.1** Composition of bath

Reagent(Chemical)	Function	Volume
Nickel Chloride Hexahydrate [NiCl <sub>2</sub> .6H <sub>2</sub> O] (Merck Life Science Pvt. Limited, Mumbai, India, No.1.93655.0521, B.N.DE9D690117,UN3288)	Act as source of Nickel	19gm/liter
Lead Nitrate[Pb(NO <sub>3</sub> ) <sub>2</sub> ] (Merck Life Science Pvt. Limited, Mumbai, India, No.–1.93669.0521,B.N. DL6D663805,UN1469,)	Act as stabilizer	0.0592gm per liter
Sodium borohydride [NaBH <sub>4</sub> ] (Merck Life Science Pvt. Limited ,Mumbai, India, No.–1949620121, B.NO. QH5Q652140, UN 1426)	Act as reducing-agent	1.82 to 2.1 gm per liter
Ethylenediamine [C <sub>2</sub> H <sub>4</sub> (NH <sub>2</sub> ) <sub>2</sub> ] (Merck Life Science Pvt. Limited, Mumbai, India, No.8.00947.0521)	Act as Complexing agent	48 to 58 ml per liter
Sodium hydroxide Pallet [NaOH] (Merck Life Science Pvt. Ltd., Mumbai, India, No.1.93502.0521, B.N.D19D692304,UN1823.)	Maintains pH (buffer)	35-40 gm/liter
Titania Dioxide Rutile [TiO <sub>2</sub> ] (Sisco Research Laboratories Pvt. Ltd. Taloja, Maharashtra, India, No.- 35299(2040319),B.N. : 3240159)	Reinforcement	0,5,10,15 gm/liter

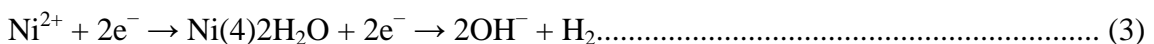
**2.2.3 Steps for the Deposition Process:**

The growth of Ni-B can be clarified by chemical reactions that occur through the deposition process. The main reactions are listed below [Srinivasan et al. 2010].

Borohydride oxidizes as the following reactions:



Corresponding reduction reactions in the coating bath can be expressed as follows:



This study used an ultrasonic assisted stirrer to create Ni-B-TiO<sub>2</sub> composite coatings with TiO<sub>2</sub> at various concentrations. Five different concentrations, 0, 5, 10, 15 and 20 gm/liter, were investigated in order to ascertain the impact of particle quantity on the composite coatings that were created. The TiO<sub>2</sub> particles utilized have a mean grain size of 500 nano meter.

Fig. 2.2 depicts the real time deposition of Ni-B-TiO<sub>2</sub> composite coating. Here 200 ml solution is taken in another 250 ml beaker and placed on a heater (IKA Laboratory Technology, Bangalore, Karnataka, India, and Model No. CRT basic) where bath temperature is raised to the deposition temperature slowly. In the bath solution, nickel chloride (NiCl<sub>2</sub>) was selected as the origin of nickel, sodium hypophosphite (NaPO<sub>2</sub>H<sub>2</sub>) as the reducing agent, Ethylenediamine as complexing agents. Lead Nitrate [Pb(NO<sub>3</sub>)<sub>2</sub>] stabilizer was introduced to avoid bath decomposition. Table 2.1 provides information on the solution bath's configuration and operational requirements. Analytical grade materials were used exclusively for this plating process. The pH meter (Eco Tester) was introduced to maintain the solution bath's pH value in between 12-14. Titania solution is added as needed. Both the temperature and the stirring frequency were maintained at 85°C and 400 rpm, respectively.

Before adding the TiO<sub>2</sub> nano particles in the solution, they were ultrasonicated for 30 minutes. During the time of coating the Ni-B deposits for the first five minutes, nano TiO<sub>2</sub> was added to the solution, and the coating process was then carried out for an additional one and half hour. Basic Ni-B coating and composite Ni-B-nano TiO<sub>2</sub> coating in absence of any surfactants were also carried out using a similar process for the aim of comparing the coating features specially in context of corrosion and scratch hardness. The coatings were then rinsed with distilled water and allowed to dry at ambient circumstances after enabling the plating to take place for the allotted amount of time.



**Fig. 2.2** Electroless Bath of Ni-B-TiO<sub>2</sub> composite coating (JU M/C Elements Laboratory)

## 2.3 MICROSTRUCTURE AND COMPOUND ANALYSIS

Detailed visual inspection of a coating is indispensable. A coating's microstructure can disclose a lot about its functional potential and serviceability. The presence of impurities and gaps between the specimen and the coating, as well as grain size and grain orientation to the specimen and other factors must be identified in order to thoroughly analyse a coating. The primary characteristics to look for in a typical coating microstructure study are (a) the coating's grain morphology with crystalline phase, (b) the substrate's grain structure and crystalline phase directly beneath the coating, (c) the coating substrate interface and (d) the coating's exterior surface. Two Scanning Electron Microscopes (SEM M/C 1 and SEM M/C 2) are used for this study which is shown in Fig. 2.3 and Fig. 2.4 respectively. This particular study has been done to examine the morphology of the plating (SEM 1) before the tribo testing and following the tribo testing by SEM2.



**Fig. 2.3** SEM M/C1 [FESEM ZEISS, \* potential - 20 kV \* working distance - 9.5 mm.]  
National Institute of Technology, Durgapur.

Since the wave length of X-rays is similar to inter planar spacing, X-ray diffraction makes use of the capability of X-rays to be diffracted by a crystalline lattice. X-ray diffraction pattern (XRD) is particularly helpful for inorganic chemical investigation since the diffraction patterns they produce are distinctive to a particular crystalline structure. This method typically makes it easy to tell apart metal oxides, nitrides, carbides, and sulfurides. It works less well with organic substances. A sample holder with rotational capability, an X-ray



source, and a number of counters to track diffracted intensity make up a diffractometer. Unlike the X-rays used in imaging, the ones employed in this procedure are monochromatic.



**Fig. 2.4** Scanning electron microscope (SEM2), make: HITACHI, model: S-3400N  
IIEST, Shibpur.

The sample is rotated to make it easier to see the diffracted pattern, which is made up of a sequence of light and dark bands that represent constructive and destructive interference between dispersed X-rays. The compounds are identified by measuring the inter-planar spacing, which is indicated by the angle between the dark and light bands. Although thicker coatings and powder samples can also be examined using XRD, bulk samples are where it works best. This particular experiment has been made for the electroless Nickel Boron (Ni-B-TiO<sub>2</sub>) coating compound analysis. This study makes use of an X-ray diffraction analyzer (Bruker D8 ADVANCE), which is depicted in Fig. 2.5.



**Fig. 2.5** D-8 advanced X-Ray diffraction machine, National Institute of Technology, Durgapur

## **2.4 SCARTCH TEST**

A scratch tester (DucomTR-101-IAS, India) in Fig. 2.6 was introduced to measure the scratch hardness. Testing was carried out under constant loads of 20 newton, 30 newton and 40 newton. The samples are scratched with a diamond indenter of the Rockwell C-type. The diamond indenter has a radius of 200  $\mu$ m and a flank angle of  $120^\circ$ . With a 5mm stroke length and 0.1mm/s indentation speed, the specimen was scratched. For obtaining optical images, Scarview imaging software was employed. This study reports an average hardness of three scratches for each weight.



**Fig. 2.6** Scratch tester (TR-101-IAS), JU M/C Elements Laboratory

## **2.5 ELECTRO CHEMICAL CORROSION**

A Potentiostat from ACM Instruments Gill AC, UK, in Fig. 2.7 was conducted for the potentiodynamic polarization test. Three electrodes are used in this test: a working electrode (sample), a saturated calomel electrode (reference electrode), and a platinum electrode (counter electrode). A voltage of between -250 mV and +250 mV is being applied. The 3.5 wt. % NaCl solution was used to corrode a 1 cm<sup>2</sup> region of the samples. Throughout the test, a 1mV/s scanning speed was maintained. The corrosion potential ( $E_{\text{corr}}$ ) and corrosion current density ( $I_{\text{corr}}$ ) of the samples were measured using Tafel extrapolation of the anodic and cathodic branch Schematic view is shown below in Fig. 2.8:



**Fig. 2.7** Potentiostat from ACM Instruments Gill AC, UK

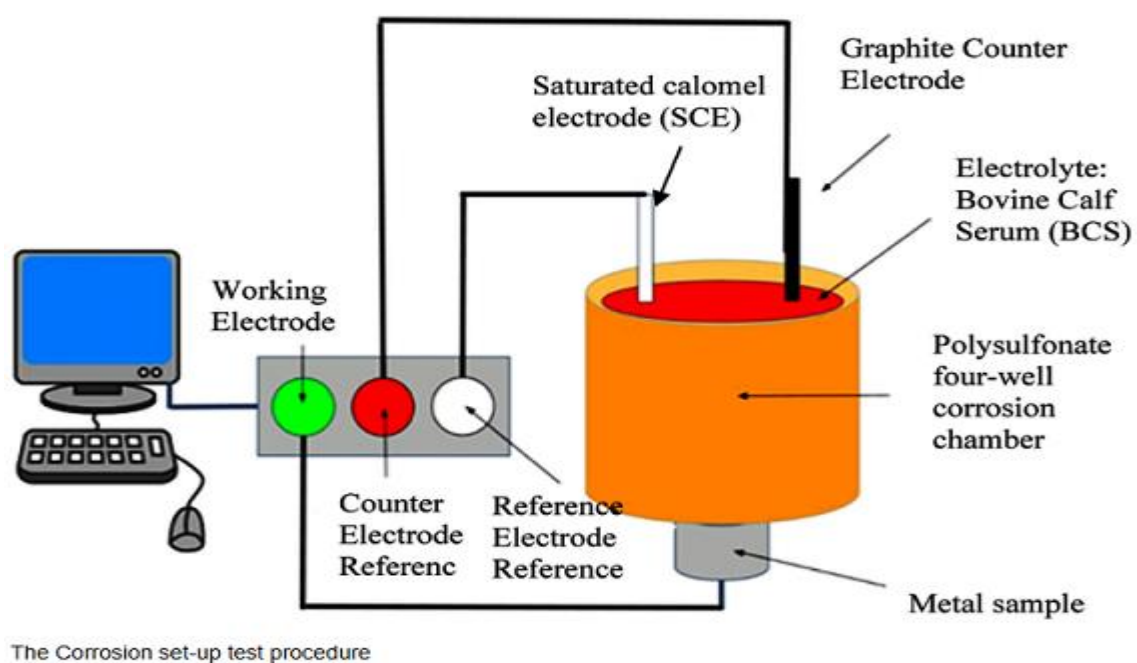


**Fig. 2.8** Schematic view of corrosion testing process diagram [Morris et al. 2021].

## **2.6 FRICTION AND WEAR TESTS**

Friction occurs between moving parts, and is commonly analyzed in parts that come into contact with one another during operation, such as power trains in automobiles. The friction causes heat generation and wear in these parts. Heat generation and wear derived from friction account for most mechanical system failures, and economic losses due to such failures are not small. To reduce such losses, tribological tests are conducted to evaluate parts and properties of the parts materials. Here the substrate tested under sequential methods and procedures like equipment used, selection of process parameters, response variables, design of experiments and analysis of variance. A detail discussion of friction and wear tests under dry condition has been carried out as follows.

### **2.6.1 Equipment used:**

The friction wear tests are carried out on a pin-on-disc type tribo tester with a computer based data collection system (TR-20LE-CHM-400, Ducom, India) at an ordinary atmospheric-temperature of approximately 36<sup>0</sup>C. The applied normal load, sliding speed and sliding duration (sliding distance) are all subject to change. The track's diameter, 80mm, is fixed. Fig. 2.9 displays a schematic representation of the tribo tester apparatus. The provided connection is used to keep the cylindrical Ni-B-TiO<sub>2</sub> coated specimens still. It exerts pressure on a 165 mm x 8 mm spinning counter face disc. The regulatory gadget included with the tribo tester can be used to regulate the speed and duration for which the disc revolves. Dead weights are added to the loading pan, which is joined to a loading lever that applies a 1:1 transmission of the normal load to the specimen, the normal load is applied. The specimen's experience of frictional force is obtained by the load cell. The displacement of the specimen is expected using an LVDT (Linear Variable Differential Transformer), which provides a clear picture of the level of wear the specimen has experienced. On the computer screen, it is expected that real time charts of wear and frictional force are displayed as they are automatically recorded. Here the amount of wear measured by the weigh balance.



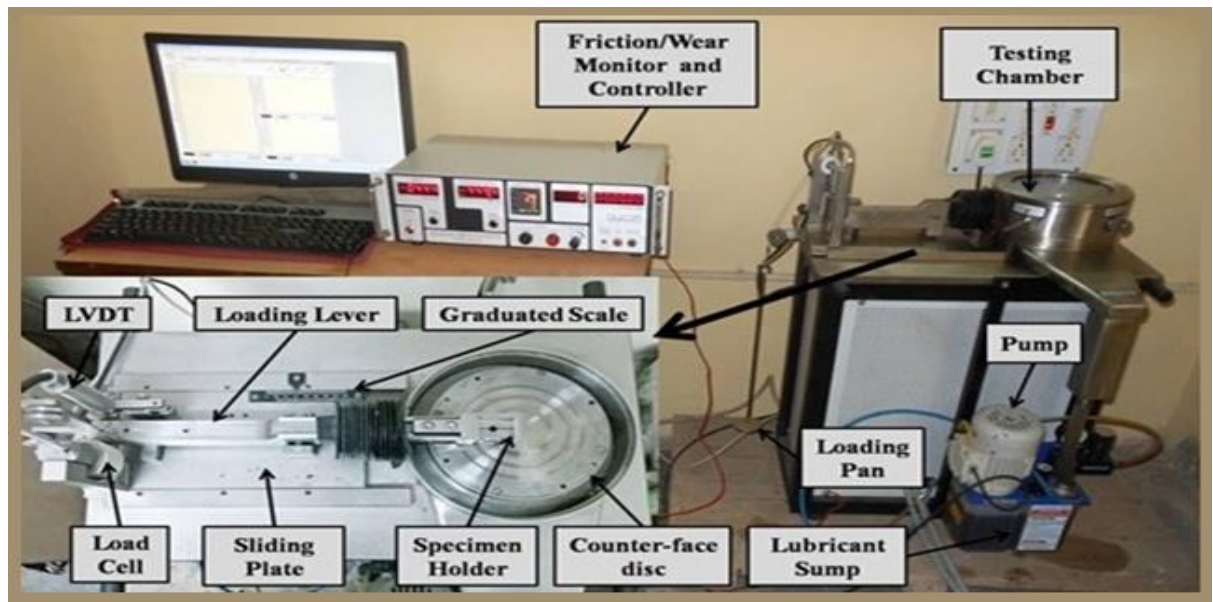


**Fig. 2.9** POD (Pin-on-disk) tribological tester (Model: TR-208-M2, Make: DUCOM)

### 2.6.2 Selection of process parameters:

Table 2.2 displays the design factors and their levels. The load, speed, sliding distance, temperature at which the test is run, the counter face disc's track diameter, and other test factors all have an impact on the tribological efficiency of electroless Nickel Boron (Ni-B) coating. But after conducting a thorough analysis of the literature to regulate the tribological characteristics of electroless Nickel-Boron-Titania (Ni-B-TiO<sub>2</sub>) coating are the applied by different parameters like load (F), sliding speed (V) and sliding distance (S). In the current investigation, three test parameter values are taken into account. Each parameter's midpoint is regarded as the beginning condition. Amount of wear and the electroless Nickel Boron Titania (Ni-B-TiO<sub>2</sub>) coating's coefficient of friction are the output parameters.

Additionally, the friction force is visible. By dividing the frictional force by the executed normal load (F), the coefficient of friction has been calculated.

**Table 2.2** Design variables and their levels.

Srl. No.	Design Factors	Unit	Level 1	Level 2	Level 3	Level 4
1	% Nano Titania	gm/liter	0	5	10	15
2	Load (F)	Newton	5	10	15	20
3	Speed (V)	rpm	50	100	150	200
4	Sliding distance(S)	mtr	100	200	300	400

### 2.6.3 Response variables:

A system or process can be thought of as a collection of tools, techniques and other aspects that converts some input (specimen type, chemical reagent, tools, energy, labours, etc.) to outcome (deposited material quality, quantity, structure, properties etc.) that has different noticeable outcomes. Some process variables ( $x_1, x_2, \dots, x_p$ ) can be regulated, so that it can be appropriately altered to regulate the process outcomes, but some alternating variables ( $z_1, z_2, \dots, z_n$ ) are uncontrollable, meaning they cannot be controlled in any way (errors in calculating equipment, inclusions in specimen, wrong human manipulation, etc.) (Fig. 2.10).

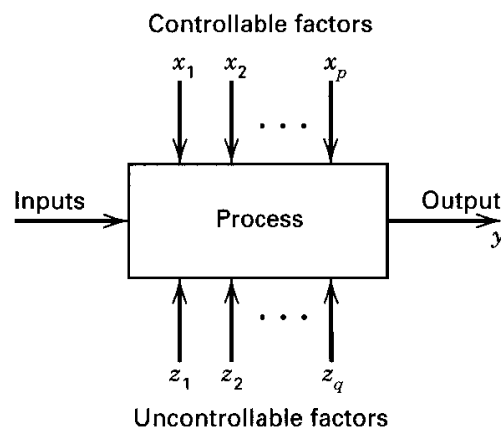


**Fig. 2.10** Process response control diagram

To find out how the controllable factors affect the response variables, deliberate modifications are performed to the controllable factors. The desired outcome is achieved with fewer trials thanks to a scientific methodology. When necessary, DOE can be quite effective (Montgomery 2014):

- ☐ Investigate how various factors affect the efficiency
- ☐ Establish the experiments with objectivity in order to solve production issues.
- ☐ maximize design of operation and its outcome
- ☐ To ascertain the degree of tolerance of the given factors.
- ☐ based on the factual information, assign resources for quality assurance.
- ☐ Investigate the effects of the various variables on performance.
- ☐ To investigate the impact of each element on system reaction.

- It will show whether or not a supplier's component poses an issue.
- How to properly blend several aspects in order to achieve the greatest outcomes.

**An effective experimental design consists of the following steps (Montgomery 2014):-**

- (i) Identification of the issue and its description.
- (ii) Choosing the output variables.
- (iii) Selection of levels and ranges of parameters.
- (iv) Selection of an experimental layout.
- (v) Carrying out the test.
- (vi) Data computation using statistics.
- (vii) Observations and suggestions.

#### **2.6.4 Design of experiments:**

It is impossible to conduct tests on a trial and error basis due to the restricted resources that are accessible and the cost effectiveness linked to a product. The entire process must be planned with a strong and effective experimental design in order to minimize the number of trials. Design of Experiments (DOE) is the name given to this strategy. It is a methodical approach to figuring out the connection between the inputs and outputs of a process. In other words, it's employed to identify cause and effect connections. To manage process inputs and maximize output, this information is required. Additionally, it offers a useful method for determining how the variables that affect the experiment's outcome interact with one another.

An experiment can be designed using a variety of techniques, including factorial designs, central composite designs, orthogonal arrays, Taguchi Analysis etc. An experiment with a full factorial design may have two or more components and two or more levels. In such a design, the number of experiments required is typically expressed as  $L^n$ , where  $L$  stands for the number of levels and  $n$  for the number of factors. Without performing a full factorial design, the central composite design is helpful in response surface methods to derive a second order equation for the answers. A huge number of experiments must be run in a factorial design as the number of process parameters rises. In these situations, the shortest matrix that contains every possible combination of parameters that may be changed and the impact of their interactions analyzed is required.



Here taking into consideration of four design parameters Taguchi analysis has been made to optimize the experiments and details results have been shown in Table 2.3.

**Table 2.3** Taguchi analysis ( $L_{16}$ )

Sl. No.	% Nano TiO <sub>2</sub>	Load(N)	Speed(rpm)	Sliding Distance (mtr)
1	0	5	50	100
2	0	10	100	200
3	0	15	150	300
4	0	20	200	400
5	5	5	100	300
6	5	10	50	400
7	5	15	200	100
8	5	20	150	200
9	10	5	150	400
10	10	10	200	300
11	10	15	50	200
12	10	20	100	100
13	15	5	200	200
14	15	10	150	100
15	15	15	100	400
16	15	20	50	300

#### 2.6.5 Analysis of variance:

Analysis of variance (ANOVA) is an analysis tool used in statistics that splits an observed aggregate variability found inside a data set into two parts: systematic factors and random factors. The systematic factors have a statistical influence on the given data set, while the random factors do not. Analysts use the ANOVA test to determine the influence that independent variables have on the dependent variable in a regression study. ANOVA determines whether the groups created by the levels of the independent variable are statistically different by calculating whether the means of the treatment levels are different from the overall mean of the dependent variable. If any of the group means is significantly different from the overall mean, then the null hypothesis is rejected. In this experiment, ANOVA is performed in context of minimum wear by the Minitab 17 software system.

# RESULTS & DISCUSSIONS

*This chapter examines how the frictional forces and amount of wear of electroless Nickel-Boron Titania (Ni-B-TiO<sub>2</sub>) coating vary with executed normal load, sliding speed, various TiO<sub>2</sub> nanoparticle percentages, and sliding duration. The tribo testing parameters has been attempted to optimize for lowering the friction and wear of the coatings under dry condition. The scratch and corrosion resistance comparison between Ni-B coating and Ni-B-TiO<sub>2</sub> coating has been studied. The sample used for SEM analysis and morphological research.*

## 3.1 INTRODUCTION

This chapter deals with the different experiments as deposited of Ni-B coatings and Ni-B-TiO<sub>2</sub> composite coatings. Comparison study of surface morphology of Ni-B Alloy surface and Ni-B-TiO<sub>2</sub> composite coating surface both has been studied before and after the tribo testing by SEM analysis. In dry friction tribo testing, the variation of response variables with process parameters has been investigated and also wear mechanism has been analyzed. In the EDX spectrum the analysis of composition i.e. to confirm the plating of nickel and boron on the mild-steel specimen has been investigated. Scratch hardness test has been carried out to compare the effect of nano particles in context of the reduction of scratch width. Corrosion test and consequent corrosion potential has been found out by the Tafel curve.

## 3.2 RESULTS AND DISCUSSION

The experimental results are discussed below:

### 3.2.1 Surface morphology:

The composition (structure and morphology) of composite coatings made of Ni-B and TiO<sub>2</sub> Fig. 3.1 shows SEM surface and cross sectional views of the coated surfaces created using the ultrasonicated electroless process on Ni-B alloy and NiB-TiO<sub>2</sub> composite materials with

various particle concentrations. It is clear from Fig. 3.1 (a) and (b) that Ni-B alloy coatings have a cauliflower structure. It is well known, the cauliflower structure increases tribological characteristics by decreasing real contact area and lubrication [Abakay and Şen 2022; Delaunois & Lienard 2002]. Fig. 3.1 (a) and (b) depict the Ni-B alloy coating's columnar structure in cross section, while Fig. 3.1 (c) and (d) depict the surface images of the coating's cauliflower structure at various magnifications. It is obvious from the surface images that the Ni-B alloy coatings, which consist of cauliflower like structure, show a columnar structure. In both of Fig. 3.1 e and 3.1 f, shows the existence of  $\text{TiO}_2$  particles. With particle reinforcement, it is clear from looking at surface images that the cauliflower like structure starts to deteriorate, but looking at higher magnification images (Fig. 3.1 (f)), it is clear that the cauliflower like structure still exists despite degrading with particle reinforcement. Fig. 3.1 (g) and (h) display cross sectional views of Ni-B- $\text{TiO}_2$  composite-coatings. It is clear from the cross sectional pictures that  $\text{TiO}_2$  particles are present in the composite structure and display an even distribution. The  $\text{TiO}_2$  particles are represented by the dark components. Additionally, it is acknowledged that the typical coating depths of alloy and composite coatings are  $40\text{ }\mu\text{m}$  and  $44\text{ }\mu\text{m}$  respectively.

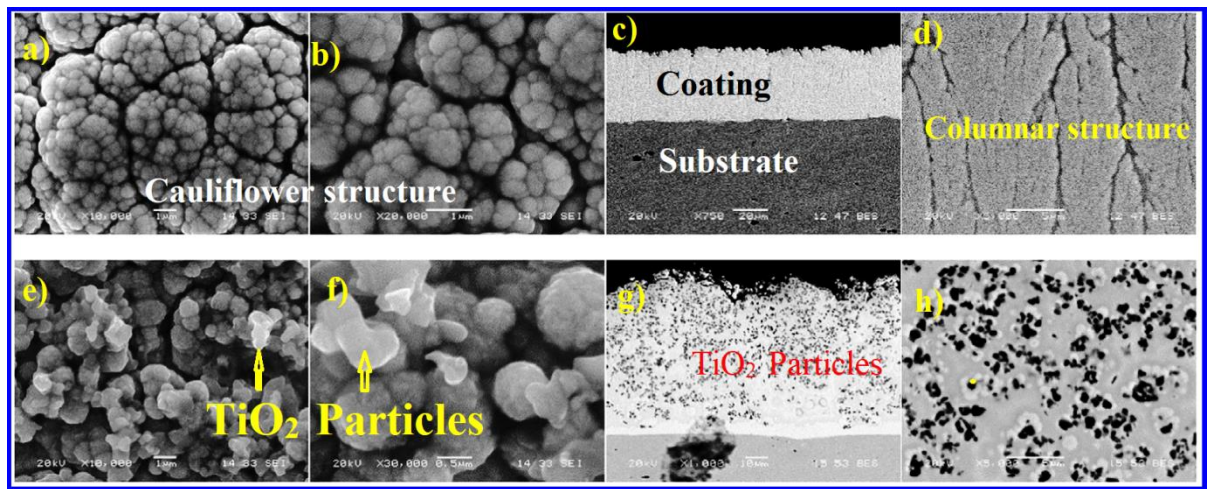


**Fig. 3.1** SEM results: surface structure (morphologies) of (i) Ni-B alloy surface: (a) and (b); cross section : (c) and (d) (ii) Ni-B- $\text{TiO}_2$  composite coating surface (e) and (f) ; cross section (g) and (h) having different magnification.

Cross sectional SEM pictures of alloy and composite coatings produced with  $\text{TiO}_2$  at different concentrations and magnifications are depicted in Fig. 3.2. Here Fig. 3.2 (a) and (b) depicts the cross sectional images of Ni-B coating without embedding  $\text{TiO}_2$  particles that exposed the columnar form of coatings. But Fig. c to j, in all the figures, in presence of different percentage of  $\text{TiO}_2$  particles specially 5 gm per liter to 15 gm per liter, shows its

existence of  $\text{TiO}_2$  with different cross sectional views.

Here for the case of 5 gm per liter nano particle (in Fig. c and d), coating exhibits small embedment of  $\text{TiO}_2$  with uneven distribution. But as the amount of particles increased to 10 gm per liter in Fig. 3.2 (e) and (f), and 15 gm. per liter in Fig. (g) and (h), uniformity of  $\text{TiO}_2$  particles increases to homogeneous distribution that showed in the cross-sectional view . In all of the above three cases the coating thickness values remarkably are measured as 40, 42 and 44  $\mu\text{m}$  respectively. Moreover, in low-magnification images it is concluded that the surface roughness increases as the  $\text{TiO}_2$  particle embedment increases.

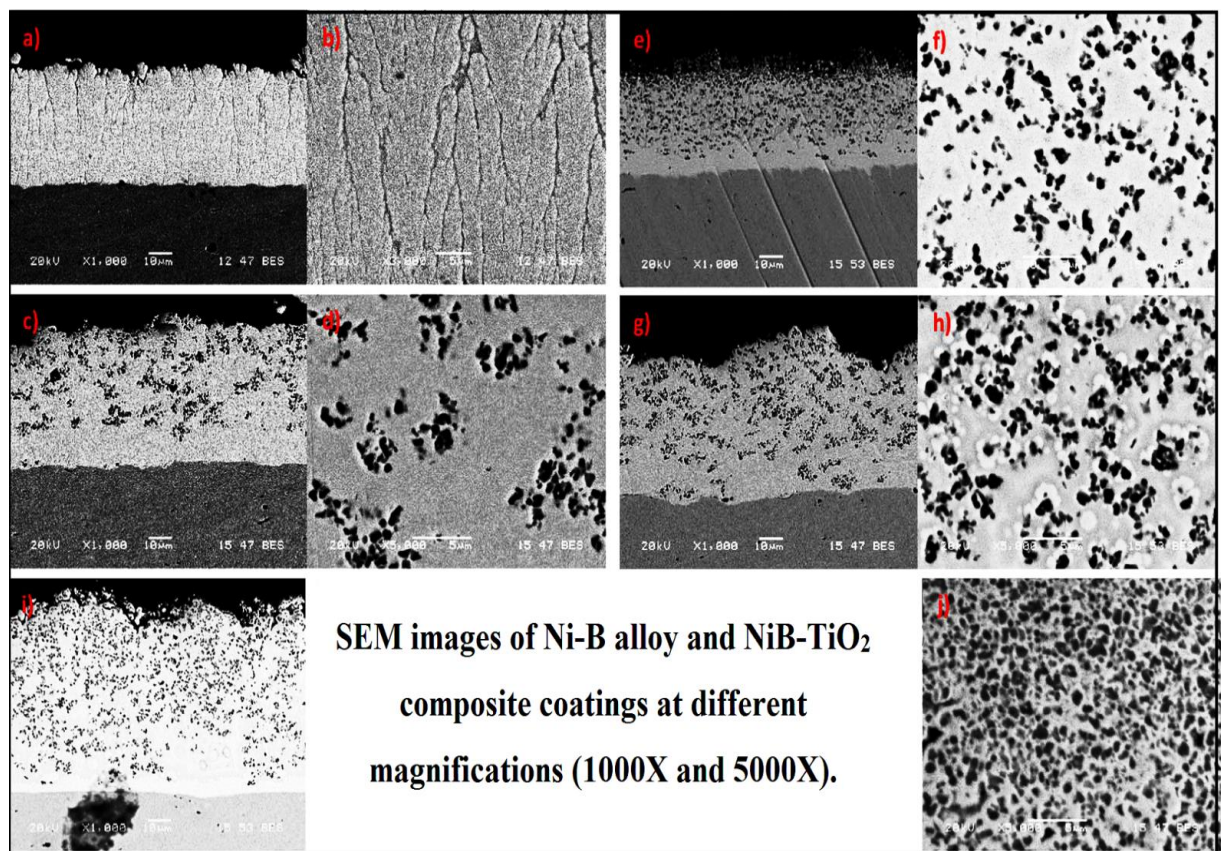


**Fig. 3.2** SEM results: images of Ni-B and Ni-B- $\text{TiO}_2$  coating at different magnification (1000X and 5000X).

### 3.2.2 Friction and wear under dry condition:

The results of wear and coefficient of friction (COF) obtained from the tribo test under dry condition have been enlisted in Table 3.1. The influence of process on friction coefficient under different combinations of parameters is analyzed. The experimental results are further processed and discussed subsequently.

**Table 3.1** Results from experiments measuring friction coefficient and weight loss at dry condition.

Sl. No	% TiO <sub>2</sub> (gm/l)	Load (N)	Speed (rpm)	Sliding Distance (m)	Duration (s)	Initial Wt. (gm)	Final Wt. (gm)	Wear (gm)	Frictional Force(N)	COF
1	0	5	50	100	636	6.6297	6.6292	0.0005	2.7	0.54
2	0	10	100	200	636	6.6292	6.6287	0.0005	5.1	0.51
3	0	15	150	300	636	6.6265	6.6245	0.0020	8.4	0.56
4	0	20	200	400	636	6.6245	6.6150	0.0095	14.2	0.71
5	5	5	100	300	955	6.6132	6.6125	0.0007	2.9	0.58
6	5	10	50	400	2547	6.6125	6.6111	0.0014	5.5	0.55
7	5	15	200	100	159	6.6237	6.6228	0.0009	8.1	0.54
8	5	20	150	200	125	6.6235	6.6227	0.0008	12.5	0.62
9	10	5	150	400	849	6.6351	6.6346	0.0005	2.8	0.56
10	10	10	200	300	477	6.6343	6.6338	0.0005	5.2	0.52
11	10	15	50	200	1273	6.5828	6.5821	0.0007	7.6	0.50
12	10	20	100	100	318	6.5819	6.5816	0.0003	10.2	0.51
13	15	5	200	200	318	6.5683	6.5680	0.0003	2.2	0.44
14	15	10	150	100	318	6.5680	6.5678	0.0002	3.9	0.39
15	15	15	100	400	1273	6.5785	6.5774	0.0011	7.3	0.48
16	15	20	50	300	1910	6.5774	6.5709	0.0065	10.1	0.50

From the above result, it is clear that as the load increases, the wear also increases. For example, in Ni-B coating without titania as the load increases from 5 N to 20 N, the wear also increases from 0.0005 gm to 0.0095 gm. But when nano particles are present, it helps to resist the wear. At 15gm/liter TiO<sub>2</sub>, as the load was 5 N the wear was only 0.0002 gm, but as the load increased to 20 N, the wear also increased to 0.0065 gm though it is less than 0.00095 gm which is obtained by 20 N and without TiO<sub>2</sub>. In sl.no.3 and 4 it is obtained that as the sliding distance as well as sliding speed increases the amount of wear also increases from 0.0020 to 0.0095.

### 3.2.2.1 Analysis of variance (ANOVA) for wear

The relevance of individual process parameters and their interactions on the system response under examination can be determined statistically using the ANOVA method. ANOVA is utilized in the current work with the goal of evaluating the applicability of testing variables

and their relations on the wear performance of electroless Nickel Boron Titania (Ni-B-TiO<sub>2</sub>) coating. When developing projection and performance model, testing variables that do not significantly affect wear can be left out or kept within suitable values of the test. ANOVA can be used to determine the variance's percentage contribution.

In this experiment, ANOVA is performed in context of minimum wear by the Minitab 17 software system with confidence level 95%. From Fig. 3.3 it is understood that to get the best result i.e. the minimum wear is performed at 10gm/liter TiO<sub>2</sub> reinforcement in the Ni-B-TiO<sub>2</sub> composite coatings. The analysis has been done i.e. the amount of wear is performed by varying the nano percentage particles, load, speed and sliding distances. From Fig. 3.3, it is obvious that wear increases as the load is increased from 5 Newton to 20 Newton and which is practical as per the mechanical properties is considered. It is also seen that a moderate speed of 100 rpm leads the minimum wear. Results also show that as the sliding distances increases the amount of wear is also increased. In Fig. 3.4 an interaction plot of wear has been shown where all the responsible parameter for the wear works together. Here it is shown that in the absence of nano particles maximum wear takes places and no sooner the nano particle is reinforced, it resist wear whatever the other parameters works . 10 gm /liter TiO<sub>2</sub> in the Ni-B-TiO<sub>2</sub> composite coatings shown in green symbol depicts the minimum wear and which is the best results of the present study.



**Fig. 3.3** Analysis of variance (ANOVA) for wear



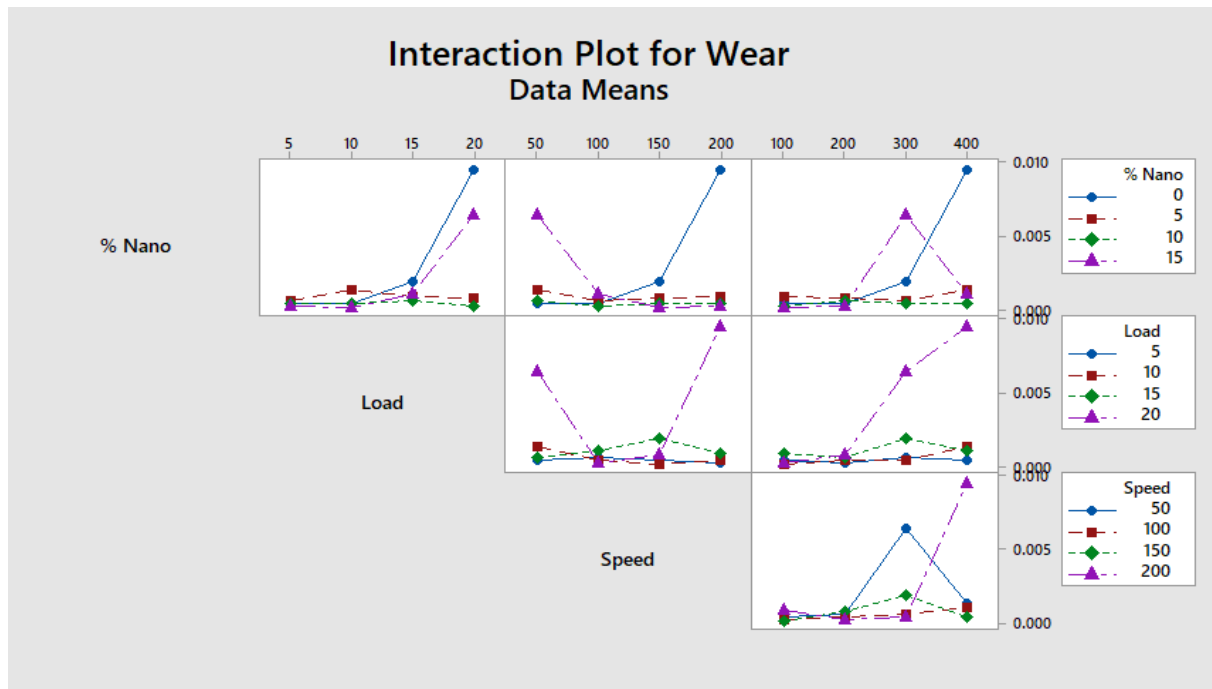


**Fig. 3.4** Interaction plot of all four tribological parameters (Nano %-Load-Speed-Sliding Distance) for wear

**Table 3.2** ANOVA analysis for wear characteristic

Source	Degree of Freedom	Sum of squares	Mean square	F-value	P-Value
Nano	3	0.000017	0.000006	1.50	0.373
Load	3	0.000038	0.000013	3.44	0.169
Speed	3	0.000013	0.000004	1.21	0.440
Distance	3	0.000021	0.000007	1.93	0.301
Error	3	0.000011	0.000004		
Total	15	0.000100			

Table 3.2 is the ANOVA table for the analysis of testing parameters for the wear behaviour of electroless Ni-B-TiO<sub>2</sub> coating. Here on the basis of F-value the most significant parameters is applied load (F-value 3.44) others parameters are not significant at the 95 % confidence level.

### 3.2.2.2 Analysis of signal to noise ratio for wear:

Even with noise inputs, the Taguchi approach seeks to minimize the variation of statistical data in the outcomes. As a result, Taguchi technique must account for the variability within a

range of operating conditions. The variability can be easily considered if the Signal to Noise (S/N) ratio is used to convert the experimental data into a value for the best assessment rather than the mean. The Signal to Noise ratio should be optimized in order to reduce the impact of random noise components, which have a significant impact on the process-performance. In the present study S/N ratio analysis, the amount of wear serves as the performance index, and Minitab is employed for all calculations. Signal to Noise (S/N) ratio is obtained by applying ‘Lower wear the Better’ design criteria and the required equation is provided as:

$$S / N = -10\log(\sum y^2 / n) \dots \dots \dots (2)$$

here ‘y’ is the observed data and ‘n’ is the number of observations. Simply said, a design parameter with a significant variance in the signal to noise ratio across factor settings denotes that it significantly contributes to the achievement of the performance feature. When there is small difference in the signal to noise ratio across various factor values, the factors are unimportant in relation to the different aspects of performance. The major effects plot provides the ideal testing parameter combination for the least amount of wear. In Fig. 3.5, a high Mean of SN ratio approx. 66 is presented at 10 gm/liter nano particles in Ni-B-TiO<sub>2</sub> composite coatings which is the best result where relevant to noise signal is high. The results also justify the ANOVA analysis. Similarly as per as load is considered at low load condition, the desired output of Signal to Noise ratio is high. Similarly as per as speed and sliding distances is concerned the best S/N ratio justify the ANOVA analysis significantly.

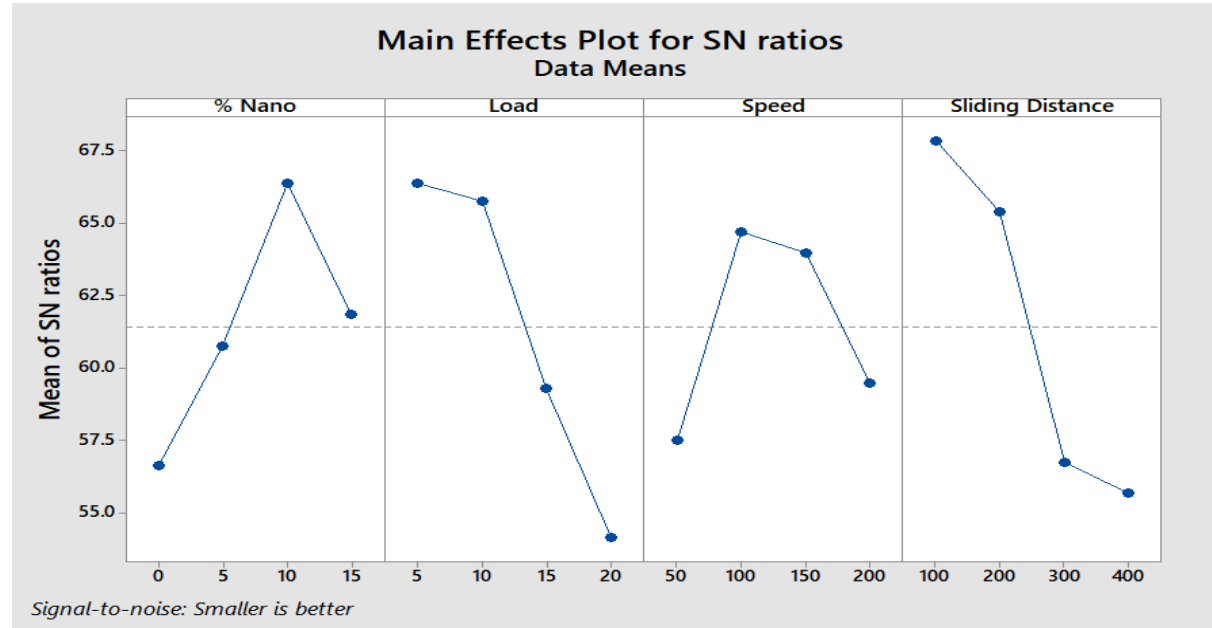


**Fig. 3.5** Signal to noise ratio for wear



From the Fig. 3.5 Signal to noise ratio for wear is obtained. Here in the S/N ratio plots it is observed that the minimum wear is obtained for 10% nano TiO<sub>2</sub>, 5 Newton load, Sliding speed 100 rpm and sliding distance of 100 mters. So may conclude these results are the optimum values for minimum wear for the present work.

### 3.2.2.3 Analysis of variance (ANOVA) for friction:

To get the minimum COF, ANOVA is performed from the experimental results. The analysis has been done by varying the nano percentage particles, load, speed and sliding distances. From the Fig. 3.6, it is understood that to get the best result i.e. the minimum COF is performed at 15 gm /liter TiO<sub>2</sub> reinforcement in the Ni-B-TiO<sub>2</sub> composite coatings. Again as load is one of the important parameter, it is observed that minimum COF is found out at 10 N load. Again the best COF results are obtaining at 100 meter sliding distance and 100 rpm. In Fig. 3.7 an interaction plot of COF has been shown where all the responsible parameter for the wear works together. Here it is understood that as the amount of TiO<sub>2</sub> decreases the COF is high and as the load increases the COF also increases.

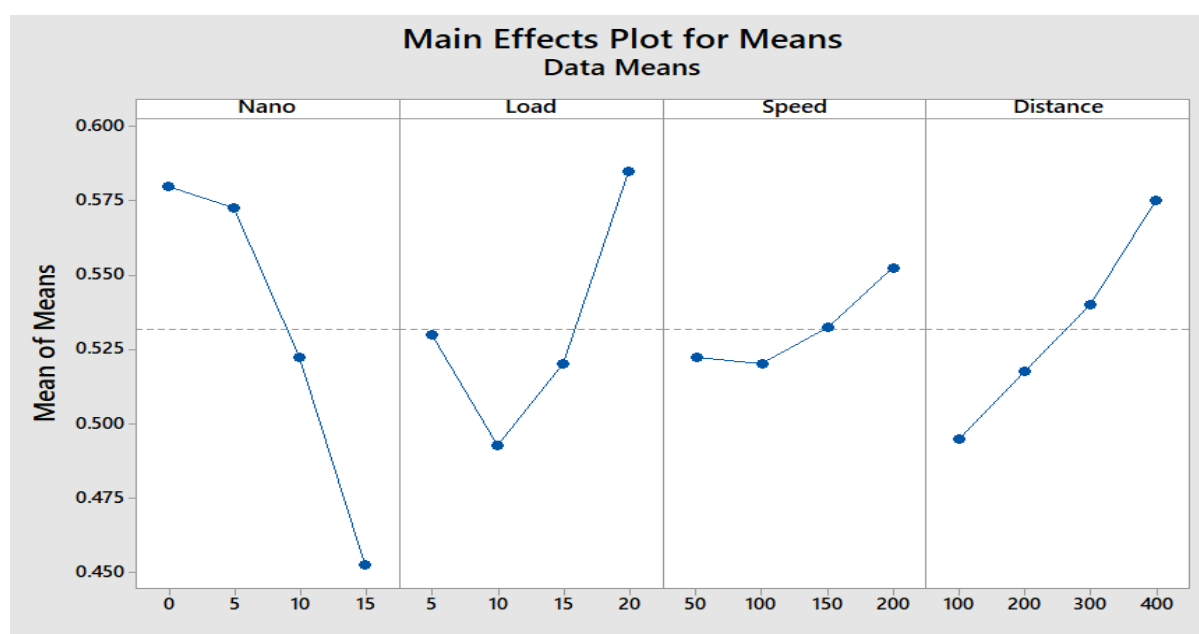


**Fig. 3.6** Analysis of variance (ANOVA) for COF

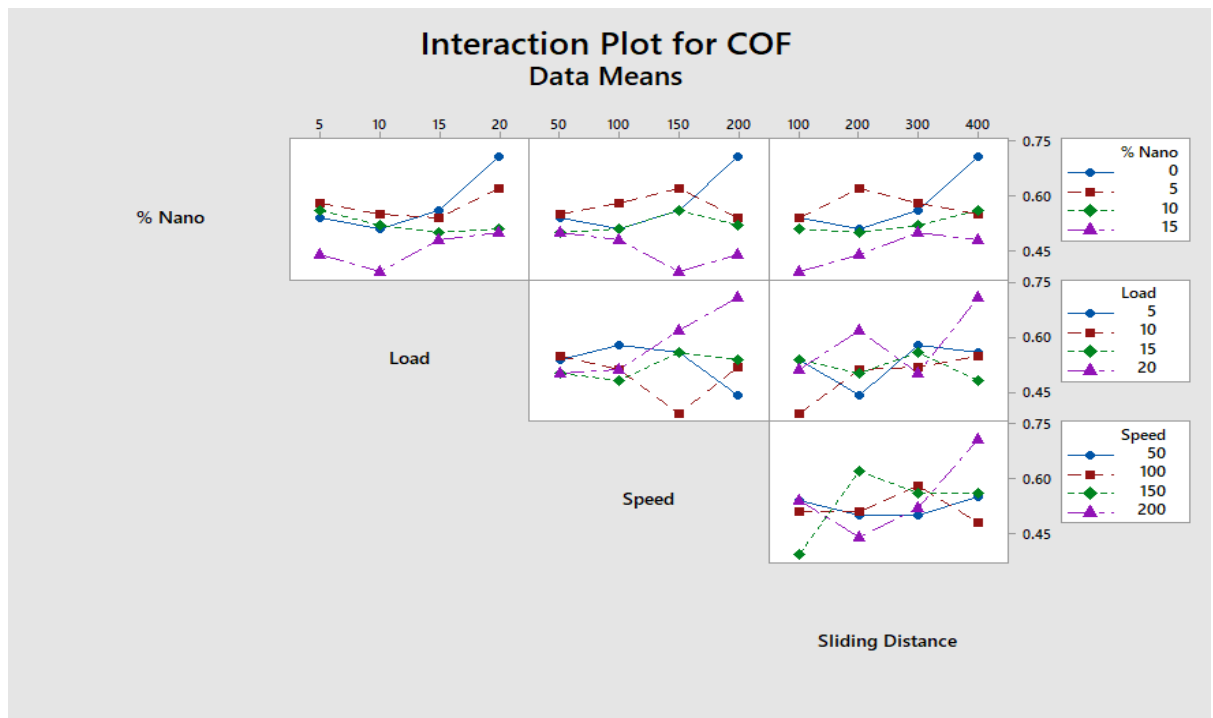


**Fig. 3.7** Interaction plot of all four tribological parameters (Nano %-Load-Speed-Sliding Distance) for COF

**Table 3.3** ANOVA analysis for friction characteristic

Source	Degree of Freedom	Sum of squares	Mean square	F-value	P-Value
Nano	3	0.041419	0.013806	19.10	0.019
Load	3	0.018069	0.006023	8.33	0.058
Speed	3	0.002619	0.000873	1.21	0.440
Distance	3	0.013969	0.004656	6.44	0.080
Error	3	0.002169	0.000723		
Total	15	0.078244			

The ANOVA analysis which is conducted on 95% confidence level, all the test parameters for the friction behaviour of electroless Ni-B-TiO<sub>2</sub> is shown in the Table 3.3. Here on the basis of F-value the most significant parameters is percentage of nano particles (F- value 19.10) followed by load and sliding distances.

#### 3.2.2.4 Analysis of signal to noise ratio for friction:

In Fig. 3.8 the signal to noise ratio for COF is obtained. Here as per the S/N ratio plots it is observed that the minimum friction is obtained for 15 % nano TiO<sub>2</sub>, 10 newton load, sliding speed 100 rpm and sliding distance of 100 meters. So we may conclude these results are the optimum values for minimum COF for the present work.

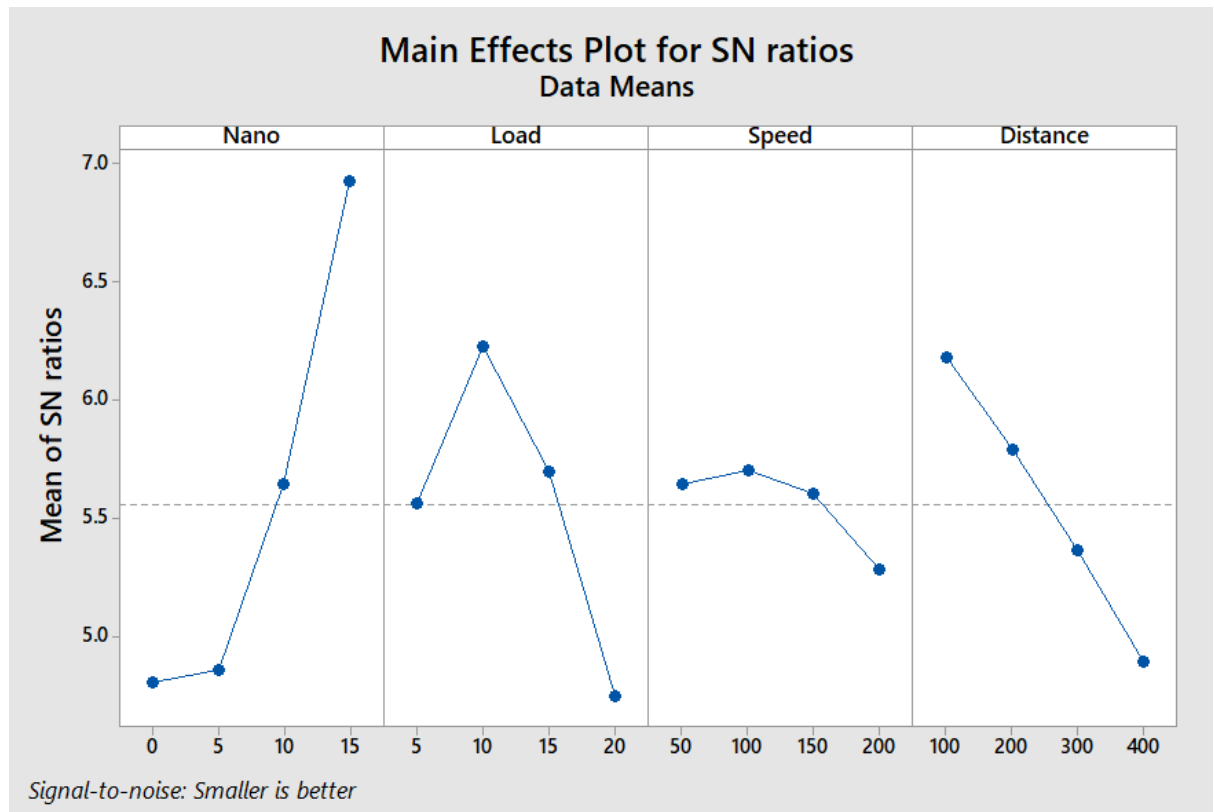


**Fig. 3.8** Signal to noise ratio for COF

### 3.2.3 Microstructural Analysis:

The pictures of the Ni-B and Ni-B-TiO<sub>2</sub> (1gm per litre) plating taken with a field emission scanning electron microscope (FESEM) are shown in Figs. 3.9(a) and (b). A typical microstructure resembling a cauliflower is shown in both pictures. The morphology of the Nickel-Boron coating as it was deposited reveals much porosity. Agglomerated nanoparticles are shown covering the pores in Fig. 3.9(b). The altered mechanical properties are caused by these implanted nanoparticles. Many publications have noted the composition and the structure of ENi plating is distinctive. Pd<sup>2+</sup> supplies nucleation sites and stimulates the specimen surface. Due to this, nodules develop and spread in a columnar pattern [Vitry et al. 2022]. The morphology that resembles a cauliflower also has tribological applications since it reduces contacting surfaces [Arias et al. 2019]. The mean nodule size for deposited Nickel-Boron and Nickel Boron Titania are 1.03 micro meters and 0.78 micro meters respectively. It depicts the refining nodule for the reason of nanoparticles.

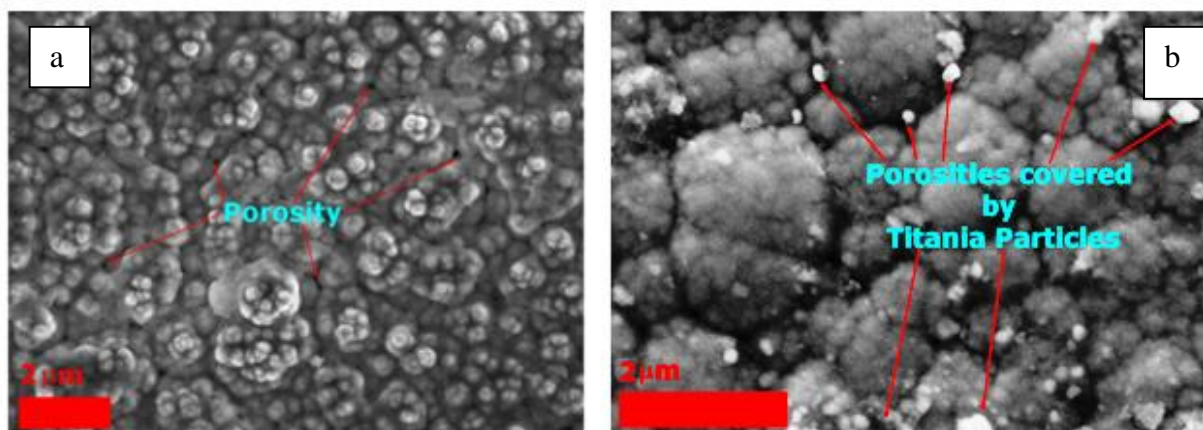


**Fig. 3.9** SEM imaging: (a) deposited Ni-B coating (b) Ni-B-TiO<sub>2</sub> (1 gm per liter)

Fig. 3.10, palladium is present in the EDAX scan, indicating that it has been utilized as a surface activator. The EDAX depicts an even distribution of TiO<sub>2</sub> noticeable in the Ni distributed zone as in Ti. Ultrasonication is the cause of the even dispersion of TiO<sub>2</sub>.

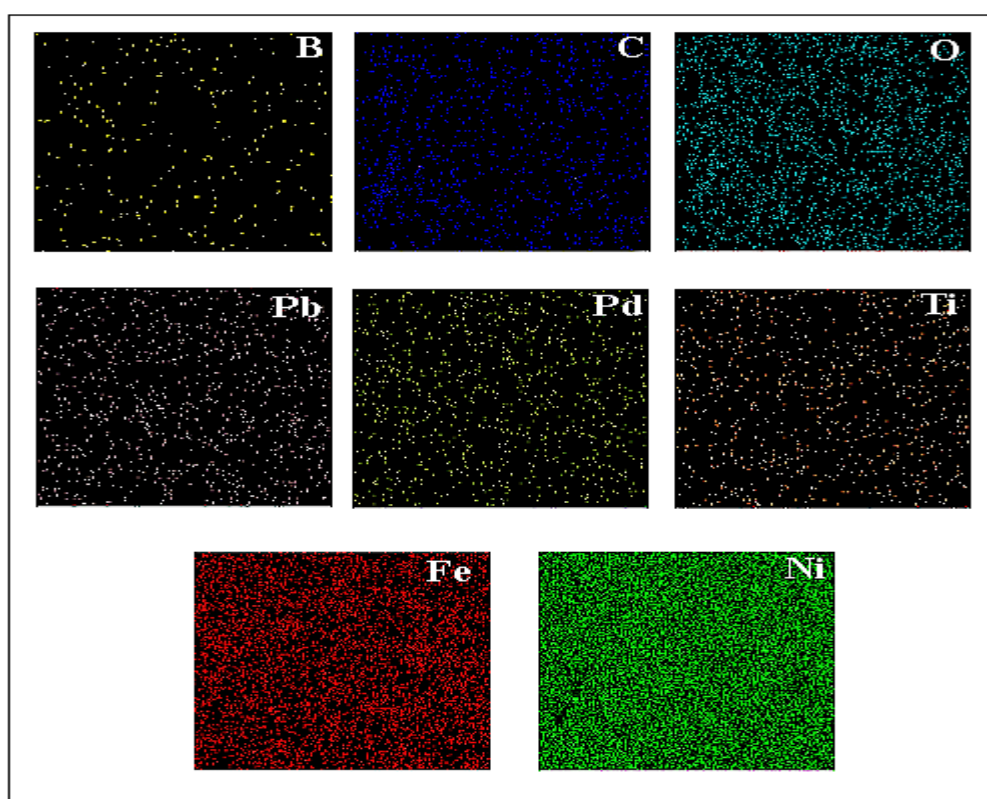


**Fig. 3.10** Nickel-Boron-TiO<sub>2</sub> deposition elemental distribution as seen by EDAX region scans.

The titania particles could present mixture all over the coating operation without any sediments because ultrasonication made it easier for a colloidal solution to form. The homogeneous dispersion of the nanoparticles is one of the main pre requisites for a sound coating with reinforced  $\text{TiO}_2$  particles. The SEM photos clearly show that the same has been accomplished in the current study.

### 3.2.4 Post tribo test surface morphology analysis:

From the Taguchi analysis, tribo test has been made considering four different parameter namely Titania (nano gm/liter) –Load (L, in newton)- Speed (S, in rpm)-Sliding Distance (D, in meter). In SEM it is found different types of results which may be in comparison significantly. In Fig. 3.11 it is found that considering other parameters in account it is very much vivid that nano particle resists the crack growth during the tribo testing.

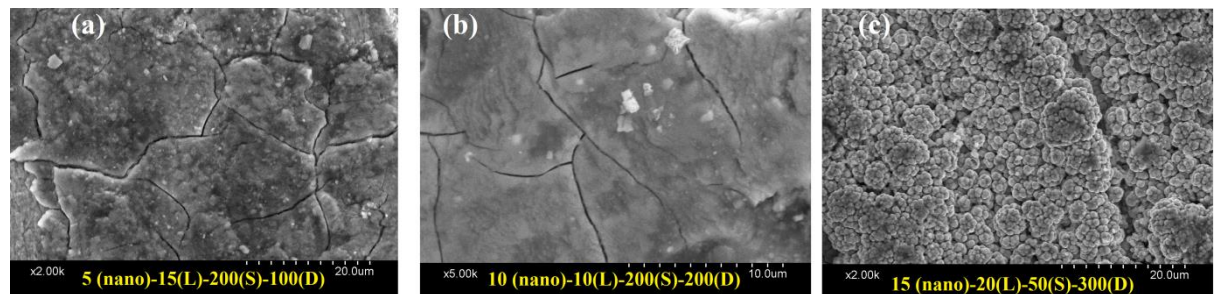


**Fig. 3.11** Post tribo test crack structure: crack arrests as nano particles increases in (a), (b),(c) respectively.

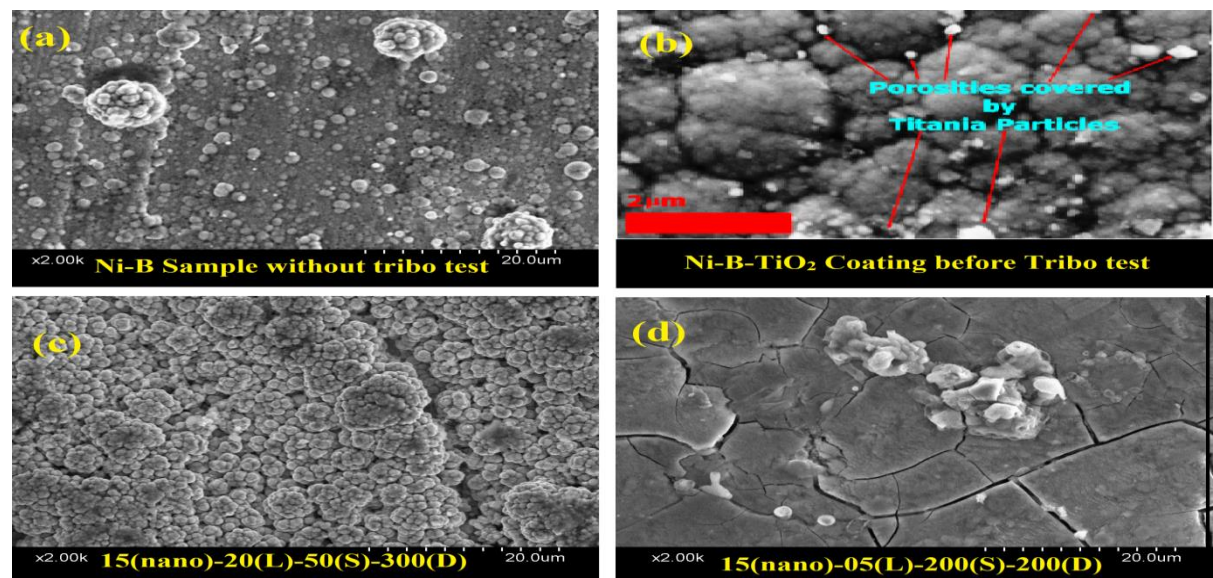


**Fig. 3.12** (a),(b) Surface morphology before tribo test Ni-B as well as Ni-B- $\text{TiO}_2$  composite. (c),(d) surface morphology after tribo test Ni-B- $\text{TiO}_2$  composite with load 20N and 5 N respectively



In Fig. 3.12 in comparison of (d) and (c) it is found that increasing load ( 5 N to 20 N) keeping nano particle percentage same (15gm/liter), the effect of nano particles disappeared as the load increases due to the fact that at high load nano particle try to absorb the load and it diminishes . In this context 3.12 (a) and (b) is a comparison in between the non-existence of nano particles (Ni-B coating) in Fig. 3.12 (a) and existence of nano particles (Ni-B-TiO<sub>2</sub>) in Fig 3.12 (b)

### 3.2.5 Scratch test:

Different scratch on Ni-B as well as Ni-B-TiO<sub>2</sub> plating is shown in Fig. 3.13(a) and (b), respectively. The distinction of bar graph measures of scratch hardness of the specimen represented in the Fig 3.14. In comparison of Nickel-Boron, Nickel-Boron-TiO<sub>2</sub> has much more scratch hardness values shows as per the applied load of 20 newton, 30 newton and 40 newton. The existence of hard TiO<sub>2</sub> nanoparticles, which are found to be embedded in the Nickel-Boron matrix after deposition, may be the cause of this. Narrow scratch is the result of these hard particles acting as a barrier to penetration.

From the equation1, the scratch-hardness is computed [Sundararajan and Roy 2011]:

$$H_s = \frac{8}{1000 \pi} \frac{F_N}{w^2} \quad (1)$$

Where,  $F_N$  (Newton) = normal load, scratch hardness =  $H_s$  (GPA) and scratch-width=  $w$  (mm)

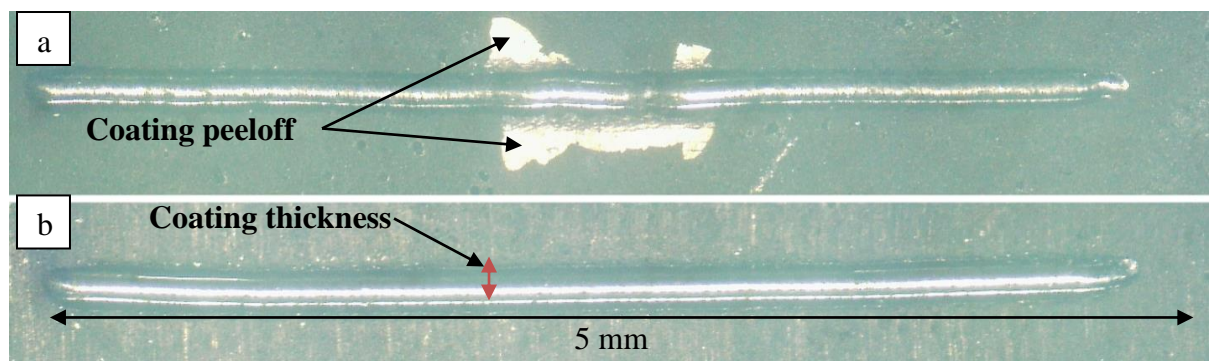


**Fig. 3.13** Scratch optical images: (a) nickel boron (Ni-B) and (b) Ni-B-TiO<sub>2</sub> composite coatings experimented at a load of 30 newton, stroke length of 5 mm and scratch speed of 0.1 mm per second.

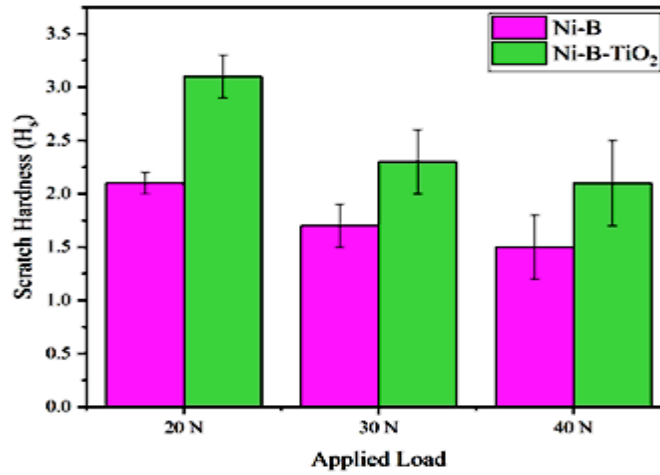


**Fig. 3.14** Bar graph: scratch resistance (/hardness) of Ni-B and Ni-B-TiO<sub>2</sub> at various loads.

Scratch hardness is inversely proportionate to (scratch width)<sup>2</sup>, hence a little change in scratch width corresponds to a high value of scratch-hardness that shows in eq<sup>n</sup>. 1. As deposited Nickel Boron exhibits coating peel off in Fig. 3.13 (a), which is shown by a bright white patch; however, Nickel-Boron-TiO<sub>2</sub> coatings do not exhibit this phenomenon (Fig. 3.13 (b)). The nano incorporation in the coatings' underside frequently act as load-bearing elements in composite in electroless Ni-B coatings and aid in distributing the applied load. This enables the energy generated by the diamond indenter's penetration and movement during scratching to be dissipated. The energy generated by the given load residue confined in the immediate area in the case of the Nickel-Boron coatings because load transfer is not promoted by the presence of nano particles. As a result, the covering starts to peel off, letting the extra localized energy out. In comparison to Ni-B, Ni-B-TiO<sub>2</sub> noticed better scratch-hardness due to the presence of the reinforcement that shows in Fig. 3.14 Very significant results shows as we applied three loads (20N, 30N and 40N) in both the coatings i.e. Ni-B and Ni-B-TiO<sub>2</sub>, a set of different scratch-hardness exhibits. For Ni-B coatings the set of scratch-hardness is (2100 MPa, 1700 MPa, and 1500 MPa) where for Ni-B-TiO<sub>2</sub> it is (3100 MPa, 2300 MPa, and 2100 MPa ) for the said load conditions 20N, 30N and 40N respectively in ideal loading circumstances.

Here in case of 20N load applied in Ni-B-TiO<sub>2</sub> coating, a nearly 48% increase in scratch hardness is observed. For 30 N and 40 N, this falls to 35% and 27%, respectively. This is due to the fact that scratch-hardness proportionate inversely on scratch width squared, so even a small amount of alteration in scratch width will have a significant impact on the samples' hardness. The comparable Ni-B-TiO<sub>2</sub> scratch width for 20N, 30N, and 40N were 128 micro

meters, 184 micro meters, and 222 micro meters, respectively. For the identical set of loads, the Ni-B coating's scratch width was greater, measuring 156  $\mu\text{m}$ , 214  $\mu\text{m}$ , and 257  $\mu\text{m}$  respectively.

### 3.2.6 Corrosion test:

Due to the rapidity with which results may be obtained, corrosion analysis using electrochemical techniques like the potentiodynamic polarization technique is becoming more and more popular. However, time consuming weight loss techniques like the salt spray technique can be useful in certain circumstances. Therefore, electrochemical techniques are better suited for laboratory studies. In this instance, a potentiostat was used to conduct the electrochemical corrosion investigation.

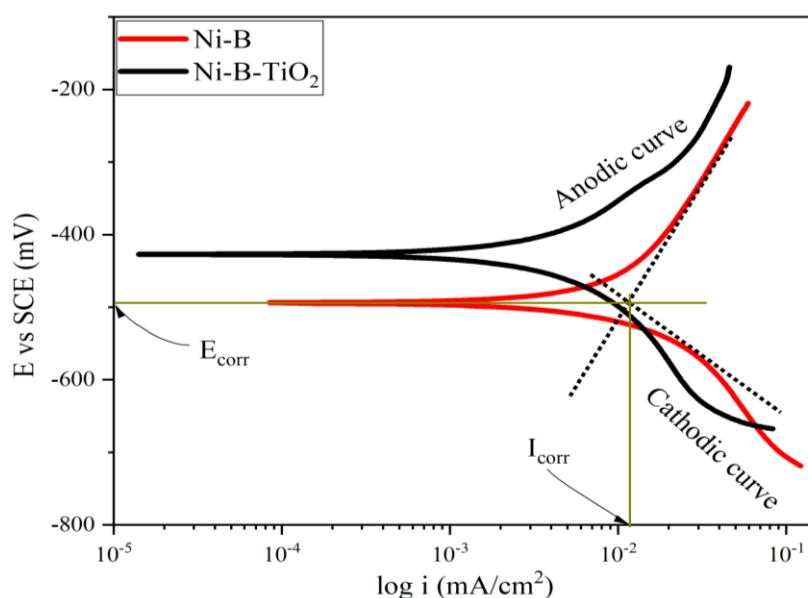


**Fig. 3.15** Tafel curve: in favor of deposited specimen.

In Fig. 3.15, in tafel plot, vertical axis electrode potential verses saturated calomel electrode and horizontal axis it is current density ( $\text{mA}/\text{cm}^2$ ). So, if corrosion goes in positive side it is more corrosion resistance and if goes negative sides it is active to the corrosion. Here two curves we are getting, upward increasing curve or anodic and downward decreasing curve i.e. cathodic curve. When both the tangent of the curve (in the steady decreasing and increasing portion) meets, a significant points derived which is corresponds to vertical axis as  $E_{\text{corr}}$  i.e. corrosion potential and corresponding horizontal axis as  $I_{\text{corr}}$  i.e. corrosion current density. In



this study, few postulates have been made to get the Tafel curve as follows:

1. Corrosion is uniformly present in the entire sample surface.
2. The Tafel region is unique.
3. We just take into account two half-cell responses.

Fig. 3.16 plots the specimen under study Nyquist curves. Despite the fact that both coatings have a similar trend, it is shown that the Nickel-Boron-TiO<sub>2</sub> coating has a larger area under the curve than the Ni-B coating. Based on the  $R_{ct}$  (charge transfer resistance), it can be seen that the corrosion resistance of the Nickel-Boron-TiO<sub>2</sub> coatings is superior to that of the Ni-B coatings. Drawing a Randles equivalent circuit yields the  $R_{ct}$ . As an alternative,  $R_{ct}$  can be calculated by determining the diameter of a circle that has been fitted onto the Nyquist curves. In the current investigation, this method is taken into consideration when getting the  $R_{ct}$  values utilizing the ACM instruments Version five Analysis programme.

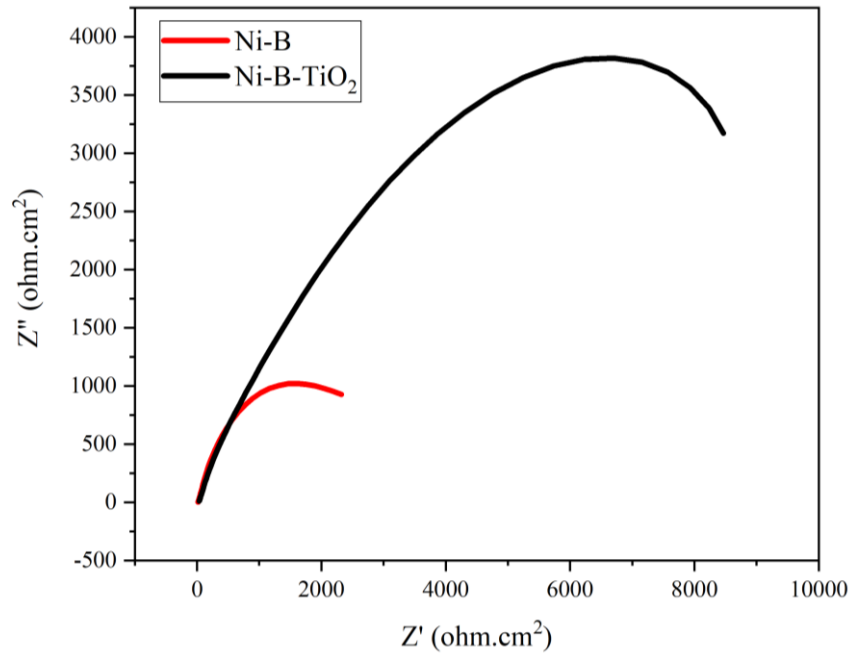


**Fig. 3.16** Nyquist plot shown in different colour for Ni-B and Ni-B-TiO<sub>2</sub> coatings.

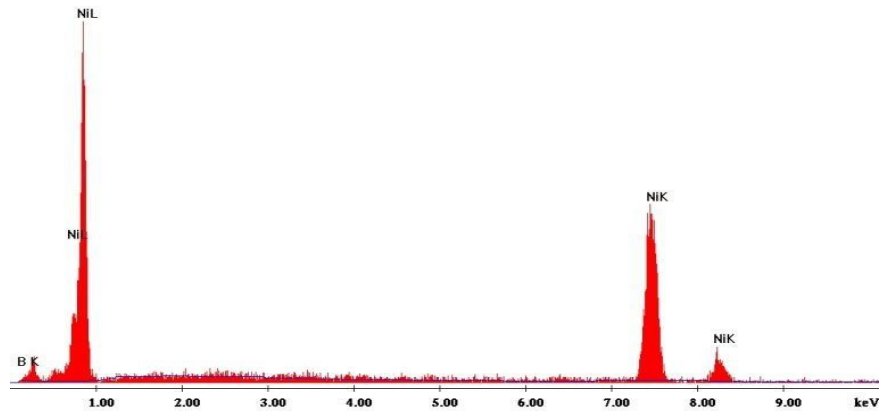
The numerical results from the polarization and Nyquist curves are displayed in Table 3.4. With the inclusion of TiO<sub>2</sub> nanoparticles, a drop in corrosion current density is seen. In the case of the Ni-B-TiO<sub>2</sub> plating,  $E_{corr}$  is likewise greater. This roughly 4-fold rise in  $R_{ct}$  value is a reliable sign of exceptional corrosion resistance. It is found that the porosity of these

coatings is coincidence with the double-layer capacitance (Cdl), as stated by the literature coatings [Ardakani et al. 2016]. Low porosity and improved surface condition are indicated by a lower Cdl. A drop in Cdl indicates that nanoparticles have gotten stuck in the spaces between nodules and have formed a seal to protect against the corrosive environment. Therefore, the corrosion of the Ni-B-TiO<sub>2</sub> coatings may be reduced by the co-deposition of nano scale TiO<sub>2</sub> coatings.

**Table 3.4** Corrosion results derived from the given tafel curves and nyquist plots

Coating Type	E <sub>corr</sub>	I <sub>corr</sub> (mA per cm <sup>2</sup> )	R <sub>ct</sub> (ohms.cm <sup>2</sup> )	C <sub>dl</sub> (F)
Ni-B	-493.84	0.00878	$3.06 \times 10^3$	$12.89 \times 10^{-5}$
Ni-B-TiO <sub>2</sub>	-427.05	0.00347	$13.79 \times 10^3$	$6.53 \times 10^{-5}$

(a)



(b)

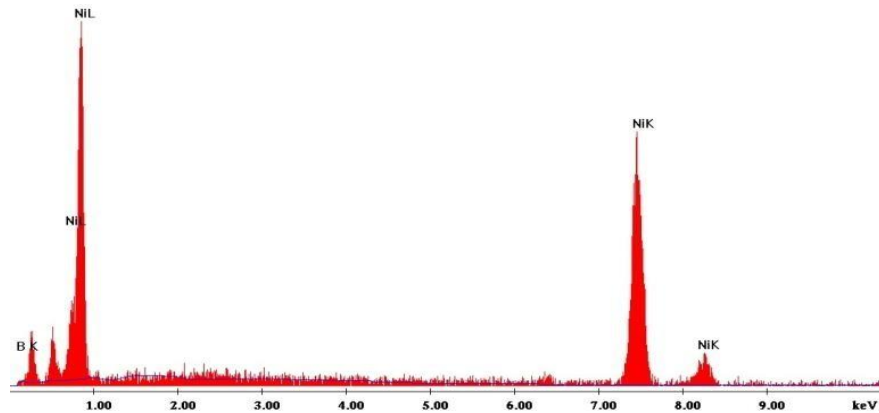


**Fig. 3.17** EDX for Ni-B coating spectrum (a) in applied deposition and (b) in heat treated (annealed at 350°C for 1hr).

### 3.2.7 Analysis of composition:

To confirm the plating of nickel and boron on the mild steel specimen, EDX is used. The EDX spectrums of the coated samples as well as coated with heat treated (350<sup>0</sup>C) specimen are shown in Fig. 3.17(a) and Fig. 3.17(b) respectively. The crest of the nickel and boron are quite specific. The boron content is seen to vary between 5.42-7.51 percent by weight. The remaining is mostly nickel.

4.8% Boron is present, according to the EDAX spectra in Fig. 3.18. Ni-B electroless TiO<sub>2</sub> coating typically has a boron concentration of 0.5 weight percent to 10 weight percent [Vitry et al. 2021]. According to Vitry et al. (2019) a borohydride reduction bath can only deposit a layer of up to 8% boron. As a result, the current coating, which contains 4.8% boron, may be considered a medium boron coating.

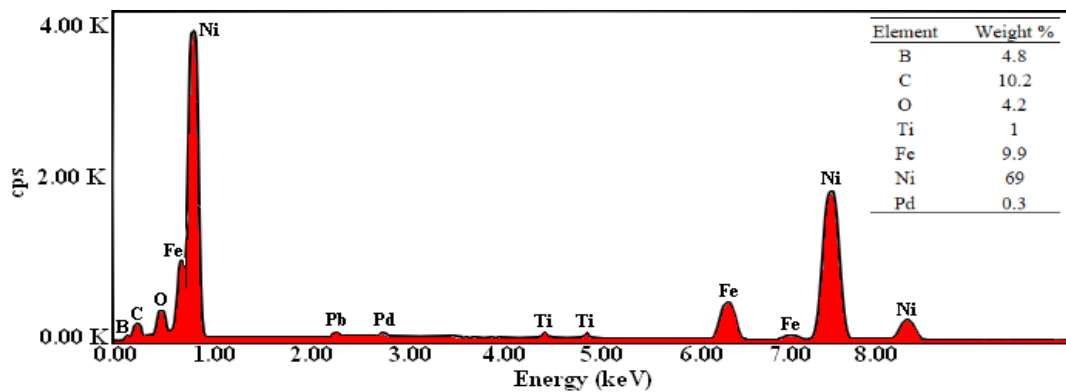


**Fig. 3.18** EDAX spectra for Ni-B-TiO<sub>2</sub> coatings

### CONCLUSIONS AND FUTURE SCOPE OF WORK

*The key findings that can be inferred from the current work are outlined in this chapter, along with the potential future directions for the research.*

#### 4.1 CONCLUSION

For the current study, samples of Ni-B and Ni-B-TiO<sub>2</sub> were produced electrolessly. Scanning Electron Microscopy and Energy Dispersive X-ray Spectroscopy both are utilized to characterize the coatings before and after the tribo testing. In the EDX spectrum the analysis of composition i.e. to confirm the plating of nickel and boron on the mild-steel specimen has been investigated and compared with the heat treated specimen. In this experiment, ANOVA is performed in context of minimum wear and COF by the Minitab 17 software system. The analysis has been done i.e. the minimum amount of wear is performed by varying the nano percentage particles, load, speed and sliding distances. It is also seen that a moderate speed of 100 rpm leads the minimum wear. Results also show that as the sliding distances increases the amount of wear is also increased. Scratch hardness test has been carried out to compare the effect of nano particles in context of the reduction of scratch width. With the inclusion of TiO<sub>2</sub> nano particles, a drop in corrosion current density is seen. The corrosion of the Ni-B-TiO<sub>2</sub> coatings is reduced by the co-deposition of nano-scale TiO<sub>2</sub> coatings.

The main findings are listed below:

- # The result was a good coating with evenly spaced nano particles.
- # Almost 20% refining of nodule is observed in the stance of Ni-B-TiO<sub>2</sub>..
- # As per the tribo testing results and consequent Taguchi Analysis, it is found that as deposited Ni-B with 10 g/l nano TiO<sub>2</sub> coating exhibits the most balanced wear properties of all the coatings under consideration and is also the most corrosion

resistant in the 3.5% NaCl environment.

# From the S/N ratio plots it is observed that the minimum friction is obtained for 15 % nano TiO<sub>2</sub>, 10 newton load, sliding speed 100 rpm and sliding distance of 100 meters.

# Ni-B-TiO<sub>2</sub>'s scratch resistance rose by roughly 48percentages for a twenty Newton load.

# The results for  $E_{\text{corr}}$  and  $I_{\text{corr}}$  are respectively, -421.02 mV and 0.00260 mA/cm<sup>2</sup>.

# Compared to Ni-B coatings, the corrosion current density of Ni-B-TiO<sub>2</sub> coatings dropped by almost 2.5 times.

#with the inclusion of nano titania particles,  $C_{\text{dl}}$  was cut in half. With the inclusion of nano particles, the scratch and corrosion resistance are significantly improved.

## 4.2 FUTURE SCOPE OF WORK

The present work is associated with the analysis of wear and friction of a composite-coating of Ni-B-TiO<sub>2</sub>. A comparative analysis of Ni-B as well as Ni-B-TiO<sub>2</sub> coating is also made. Scratch and corrosion tests are also made in context of the comparative analysis of Ni-B coatings and Ni-B-TiO<sub>2</sub> composite coatings.

During the process of study it is also understand that a huge amount of work till in our scope to explore. Few of them discussed below:

# Tribo testing is required to study under lubricating condition. A comparative analysis with dry tribo testing is required.

# A comparative analysis of micro hardness test is required in between Ni-B and Ni-B-TiO<sub>2</sub> composite-coating. Different type of elastic modulus analysis is required in context of different composite coatings like nano Zirconia, nano Alumina ,nano Titania etc.

# To learn more about the chemistry of the inter metallic phases that emerged from the interaction of the nano particles with the Ni-B matrix, **Heat Treatment** study of these nano composite coatings are mostly desirable in the future study.

# For the research of wear and frictional-coefficient, **additional test parameters**, such as lubricant flow rate, type of lubricant, different type of load like vibration load, impact load etc , test temperature, environmental factors like humidity, etc., may be included.

# Optimization of process parameters using Grey Fuzzy analysis can be considered to get

better results.

# A vast study and consequent coatings process can be developed in different industry demand materials like **Magnesium and Aluminum alloy coatings** instead of Ni-B-TiO<sub>2</sub> coatings.

# Because of their huge special features, electroless Ni-coatings are preferred for numerous engineering-applications. The operational method is difficult due to the relatively small span of bath life and variable deposit standard during the bath life. Submitted by Longfield et al. (2005) the method, known as the EDEN System for Electroless Ni Bath Life enhancement and harmonious quality, is based on the knowledge of big EN plates, one of which has achieved more than 2,000 metal turns with harmonious deposit quality. Different system may develop to ensure the practicality and longevity of the technology, as well as enable the complete assessment of the economic and environmental implications of applying EN-B coatings.

## REFERENCES

---

- A. Brenner & G. E. Riddell, Journal of Research of the National Bureau of Standards, vol. 39, 1946, pp. 385-395 and Proceedings of the American Electroplaters' Society, vol. 34, 1947, pp 156-170.
- A. Wurtz, Comptes Rendus Hebdomadaires des Séances de l'Académie des Sciences, vol. 18, 1844, pp. 702 and vol. 21, 1845, pp.149.
- Aal, A. A., Shaaban, A., & Hamid, Z. A. (2008). Nano crystalline soft ferromagnetic Ni–Co–P thin film on Al alloy by low temperature electroless deposition. Applied Surface Science, 254(7), 1966-1971.
- Abakay, E., & Şen, U. (2023). Effect of morphological and microstructural variations on the properties of electroless nickel boron coatings. Transactions of the Indian Institute of Metals, 76(3), 657-664.
- Afroukhteh, S., Dehghanian, C., & Emany, M. (2012). Preparation of the Ni–P composite coating co-deposited by nano TiC particles and evaluation of its corrosion property. Applied Surface Science, 258(7), 2597-2601.
- Agarwala, R. C., & Agarwala, V. (2003). Electroless alloy/composite coatings: A review. Sadhana, 28, 475-493.
- Aixiang, Z., Weihao, X., & Jian, X. (2005). Electroless Ni–Co–P coating of cenospheres using  $[Ag(NH_3)_2]^+$  activator. Materials Letters, 59(4), 524-528.
- Apachitei, I., Duszczek, J., Katgerman, L., & Overkamp, P. J. B. (1998). Electroless Ni–P composite coatings: the effect of heat treatment on the microhardness of substrate and coating. Scripta Materialia, 38(9), 1347-1353.
- Ardakani, S. R., Afshar, A., Sadreddini, S., & Ghanbari, A. A. (2017). Characterization of Ni–P–SiO<sub>2</sub>–Al<sub>2</sub>O<sub>3</sub> nano-composite coatings on aluminum substrate. Materials Chemistry and Physics, 189, 207-214.

Arias, S., Castaño, J. G., Correa, E., Echeverría, F., & Gómez, M. (2019). Effect of heat treatment on tribological properties of Ni-B coatings on low carbon steel: wear maps and wear mechanisms. *Journal of Tribology*, 141(9), 091601.

B. Kaya, T. Gulmez & M. Demirkol, Preparation and properties of electroless Ni-B and Ni-B nano composite coatings, in: *Proc. World Congr. Eng. Comput. Sci.*, 2008, p. 1–5.

Brooks, I., Lin, P., Palumbo, G., Hibbard, G. D., & Erb, U. (2008). Analysis of hardness–tensile strength relationships for electroformed nanocrystalline materials. *Materials Science and Engineering: A*, 491(1-2), 412-419.

Cao, Z. H., Wang, L., Hu, K., Huang, Y. L., & Meng, X. K. (2012). Microstructural evolution and its influence on creep and stress relaxation in nanocrystalline Ni. *Acta materialia*, 60(19), 6742-6754.

Charbonnier, M., Romand, M., & Goepfert, Y. (2006). Ni direct electroless metallization of polymers by a new palladium-free process. *Surface and Coatings Technology*, 200(16-17), 5028-5036.

Chen, W., Gao, W., & He, Y. (2010). Sol-enhanced triple-layered Ni-P-TiO<sub>2</sub> composite coatings. *Journal of sol-gel science and technology*, 55, 187-190.

Chen, Z., Xu, X., Wong, C. C., & Mhaisalkar, S. (2003). Effect of plating parameters on the intrinsic stress in electroless nickel plating. *Surface and Coatings Technology*, 167(2-3), 170-176.

Cheong, W. J., Luan, B. L., McIntyre, N. S., & Shoesmith, D. W. (2007). XPS characterization of the corrosion film formed on the electroless nickel deposit prepared using different stabilizers in NaCl solution. *Surface and Interface Analysis: An International Journal devoted to the development and application of techniques for the analysis of surfaces, interfaces and thin films*, 39(5), 405-414.

Chhor, K., Bocquet, J. F., & Pommier, C. (1992). Syntheses of submicron TiO<sub>2</sub> powders in vapor, liquid and supercritical phases, a comparative study. *Materials chemistry and physics*, 32(3), 249-254.

Das, S. K., & Sahoo, P. (2011). Tribological characteristics of electroless Ni-B coating and



optimization of coating parameters using Taguchi based grey relational analysis. *Materials & Design*, 32(4), 2228-2238.

Delaunois, F., & Lienard, P. (2002). Heat treatments for electroless nickel–boron plating on aluminium alloys. *Surface and Coatings Technology*, 160(2-3), 239-248.

Delaunois, F., Petitjean, J. P., Lienard, P., & Jacob-Duliere, M. (2000). Autocatalytic electroless nickel-boron plating on light alloys. *Surface and Coatings Technology*, 124(2-3), 201-209.

Dervos, C. T., Novakovic, J., & Vassiliou, P. (2004). Vacuum heat treatment of electroless Ni–B coatings. *Materials Letters*, 58(5), 619-623.

Gadhari, P., & Sahoo, P. (2016). Electroless nickel-phosphorus composite coatings: A review. *International Journal of Manufacturing, Materials, and Mechanical Engineering (IJMMME)*, 6(1), 14-50.

Gül, H. (2023). The Effect of TiO<sub>2</sub> Concentration on Morphology, Wear and Corrosion Properties of NiB-TiO<sub>2</sub> Composite Coatings by Ultrasonic-Assisted Pulse Electrodeposition. *Surface Topography: Metrology and Properties*.

Guo, Z. C., Yang, X. W., Lin, H. K., Wang, Z. Y., & Wang, M. (1997). STRUCTURE AND PROPERTIES OF RE-Ni-B-Al<sub>2</sub>O<sub>3</sub> COATING MATERIAL, 10(1), 56.

Hamdy, A. S., Shoeib, M. A., Hady, H., & Salam, O. A. (2007). Corrosion behavior of electroless Ni–P alloy coatings containing tungsten or nano-scattered alumina composite in 3.5% NaCl solution. *Surface and Coatings Technology*, 202(1), 162-171.

Hamid, Z. A., Hassan, H. B., & Attyia, A. M. (2010). Influence of deposition temperature and heat treatment on the performance of electroless Ni–B films. *Surface and coatings technology*, 205(7), 2348-2354.

Holmberg, K., & Erdemir, A. (2017). Influence of tribology on global energy consumption, costs and emissions. *Friction*, 5, 263-284.

Jiaqiang, G., Lei, L., Yating, W., Bin, S., & Wenbin, H. (2006). Electroless Ni–P–SiC composite coatings with superfine particles. *Surface and Coatings Technology*, 200(20-21), 5836-5842.

- Kamiya, K., Yoko, T., & Bessho, M. (1987). Nitridation of TiO<sub>2</sub> fibres prepared by the sol-gel method. *Journal of materials science*, 22, 937-941.
- Kamiyama, T., Yoshida, N., & Suzuki, K. (1994). A SAXS Characterization of Particle Aggregation in TiO<sub>2</sub> Sol-Gel System (Commemoration Issue Dedicated to Professor Sumio Sakka On the Occasion of His Retirement). *Bulletin of the Institute for Chemical Research, Kyoto University*, 72(2), 225-230.
- Kanani, N. (2004). *Electroplating: basic principles, processes and practice*. Elsevier.
- Kanta, A. F., Vitry, V., & Delaunois, F. (2009). Effect of thermochemical and heat treatments on electroless nickel–boron. *Materials Letters*, 63(30), 2662-2665.
- Kanta, A. F., Vitry, V., & Delaunois, F. (2009). Wear and corrosion resistance behaviours of autocatalytic electroless plating. *Journal of Alloys and Compounds*, 486(1-2), L21-L23.
- Khoperia, T. N. (2003). Investigation of the substrate activation mechanism and electroless Ni–P coating ductility and adhesion. *Microelectronic Engineering*, 69(2-4), 391-398.
- Krishnaveni, K., Narayanan, T. S., & Seshadri, S. K. (2005). Electroless Ni–B coatings: preparation and evaluation of hardness and wear resistance. *Surface and Coatings Technology*, 190(1), 115-121.
- Krishnaveni, K., Narayanan, T. S., & Seshadri, S. K. (2008). Electrodeposited Ni–B–Si<sub>3</sub>N<sub>4</sub> composite coating: Preparation and evaluation of its characteristic properties. *Journal of Alloys and Compounds*, 466(1-2), 412-420.
- Li, L., & An, M. (2008). Electroless nickel–phosphorus plating on SiCp/Al composite from acid bath with nickel activation. *Journal of Alloys and Compounds*, 461(1-2), 85-91.
- Longfield, P., Rock Hill, S., Orgill, G., Street, W., & Bromwich, W. (2005). The eden system for electroless nickel bath life extension and consistent quality. In *Proceedings–AESF SUR/FIN Annual, International Technical Conference* (pp. 99-110).
- Lopez, T., Sanchez, E., Bosch, P., Meas, Y., & Gomez, R. (1992). FTIR and UV-Vis (diffuse reflectance) spectroscopic characterization of TiO<sub>2</sub> sol-gel. *Materials chemistry and physics*,
- Mafi, I. R., & Dehghanian, C. (2011). Comparison of the coating properties and corrosion

rates in electroless Ni–P/PTFE composites prepared by different types of surfactants. *Applied Surface Science*, 257(20), 8653-8658.

Masseoud, M., Antar, Z., Fridrici, V., Barletta, M., & Elleuch, K. (2021). Tribological properties of Ni–B–TiO<sub>2</sub> sol composite coating elaborated by sol-enhanced process: abrasive wear and impact wear. *Journal of Materials Research and Technology*, 13, 857-871.

Mintab User Manual (Release 13.2), Making data analysis easier, MINTAB Inc., State College, PA, USA, 2001.

Mohanty, D., Bhowmick, A. K., Barman, T. K., & Sahoo, P. (2023). Scratch and corrosion behaviour study of electroless Ni-B reinforced with ultrasonicated nano TiO<sub>2</sub>. *Materials Today: Proceedings*.

Momenzadeh, M., & Sanjabi, S. (2012). The effect of TiO<sub>2</sub> nanoparticle codeposition on microstructure and corrosion resistance of electroless Ni-P coating. *Materials and Corrosion*, 63(7), 614-619.

Morris, D., Mamidi, S. K., Kamat, S., Cheng, K. Y., Bijukumar, D., Tsai, P. I., ... & Mathew, M. T. (2021). Mechanical, electrochemical and biological behavior of 3D printed-porous titanium for biomedical applications. *Journal of Bio-and Tribo-Corrosion*, 7, 1-15

Narayanan, T. S., & Seshadri, S. K. (2004). Formation and characterization of borohydride reduced electroless nickel deposits. *Journal of alloys and compounds*, 365(1-2), 197-205.

Narayanan, T. S., Krishnaveni, K., & Seshadri, S. K. (2003). Electroless Ni–P/Ni–B duplex coatings: preparation and evaluation of microhardness, wear and corrosion resistance. *Materials Chemistry and Physics*, 82(3), 771-779.

Narayanan, T. S., Selvakumar, S., & Stephen, A. (2003). Electroless Ni–Co–P ternary alloy deposits: preparation and characteristics. *Surface and Coatings Technology*, 172(2-3), 298-307.

Novakovic, J., Vassiliou, P., Samara, K., & Argyropoulos, T. (2006). Electroless NiP–TiO<sub>2</sub> composite coatings: their production and properties. *Surface and Coatings Technology*, 201(3-4), 895-901.

Oraon, B., Majumdar, G., & Ghosh, B. (2006). Application of response surface method for

predicting electroless nickel plating. *Materials & design*, 27(10), 1035-1045.

P. Sahoo, Fractal characterization & optimization of electroless Ni-P coatings, *Journal of Physics D-Applied Physics*, vol. 41, 2008, 025310 (9pp.)

Panja, B., & Sahoo, P. (2014).Friction performance of electroless Ni-P coatings in alkaline medium and optimization of coating parameters.*Procedia Engineering*, 97, 47-55.

Rabizadeh, T., & Allahkaram, S. R. (2011).Corrosion resistance enhancement of Ni-P electroless coatings by incorporation of nano-SiO<sub>2</sub> particles. *Materials & Design*, 32(1), 133-138.

Ranganatha, S., Venkatesha, T. V., & Vathsala, K. (2010).Development of electroless Ni-Zn-P/nano-TiO<sub>2</sub> composite coatings and their properties. *Applied Surface Science*, 256(24), 7377-7383.

Reddy, V. V. N., Ramamoorthy, B., & Nair, P. K. (2000).A study on the wear resistance of electroless Ni-P/Diamond composite coatings. *Wear*, 239(1), 111-116.

Riedel, W. (1991).Electroless nickel plating. ASM International.

S. Tien, J. Duh and Y. Chen, Structure, thermal stability and mechanical properties of electroless Ni-P-W alloy coatings during cycle test, *Surface and Coatings Technology*, vol. 177-178, 2004, pp. 532-536.

Sahoo, P., & Das, S. K. (2011).Tribology of electroless nickel coatings—a review. *Materials & Design*, 32(4), 1760-1775.

Saito, T., Sato, E., Matsuoka, M., &Iwakura, C. (1998).Electroless deposition of Ni-B, Co-B and Ni-Co-B alloys using dimethylamineborane as a reducing agent. *Journal of Applied electrochemistry*, 28, 559-563.

Sathish, M., Radhika, N., & Saleh, B. (2022). Duplex and Composite Coatings: A Thematic Review on Thermal Spray Techniques and Applications. *Materials International*, 1-69.

Sayyad, F., & Senanayake , R. (2021).Experimental investigation on surface roughness of electroless Ni-B-TiO<sub>2</sub> nano composite coatings. *Sādhana*, 46(2), 61.

Shakoor, R. A., Kahraman, R., Gao, W., & Wang, Y. (2016). Synthesis, characterization and

- applications of electroless Ni-B coatings-a review. *Int. J. Electrochem. Sci*, 11(3), 2486-2512.
- Shakoor, R. A., Kahraman, R., Waware, U., Wang, Y., & Gao, W. (2014). Properties of electrodeposited Ni-B-Al<sub>2</sub>O<sub>3</sub> composite coatings. *Materials & Design*, 64, 127-135.
- Shen Rongrong, & Xiao Jiuyi. (2007). Fretting wear behavior of Ni-B and Ni-B/BN electroless plating. *Journal of Materials Heat Treatment*, 28(3), 121-124.
- Shiue, S. T., Yang, C. H., Chu, R. S., & Yang, T. J. (2005). Effect of the coating thickness and roughness on the mechanical strength and thermally induced stress voids in nickel-coated optical fibers prepared by electroless plating method. *Thin Solid Films*, 485(1-2), 169-175.
- Song, Y. W., Shan, D. Y., & Han, E. H. (2008). High corrosion resistance of electroless composite plating coatings on AZ91D magnesium alloys. *Electrochimica Acta*, 53(5), 2135-2143.
- Srinivasan, K. N., Meenakshi, R., Santhi, A., Thangavelu, P. R., & John, S. (2010). Studies on development of electroless Ni-B bath for corrosion resistance and wear resistance applications. *Surface Engineering*, 26(3), 153-158.
- Sudagar, J., Lian, J., & Sha, W. (2013). Electroless nickel, alloy, composite and nano coatings—A critical review. *Journal of alloys and compounds*, 571, 183-204.
- Sun, W. C., Zhang, P., Zhao, K., Tian, M. M., & Wang, Y. (2015). Effect of graphite concentration on the friction and wear of Ni-Al<sub>2</sub>O<sub>3</sub>/graphite composite coatings by a combination of electrophoresis and electrodeposition. *Wear*, 342, 172-180.
- Sundaraj, M., & Subramani, V. (2021). Influence of N-Dodecyl Betaine Surfactant on Electroless Ni-P-nano-ZnO<sub>2</sub> Composite Coating Properties Prepared on Magnesium AZ91D Alloy. *International Journal of Electrochemical Science*.
- Sundararajan, G., & Roy, M. (2011). Hardness testing. *Encyclopedia of Materials: Science and Technology*, 3728-3736.
- Terabe, K., Kato, K., Miyazaki, H., Yamaguchi, S., Imai, A., & Iguchi, Y. (1994). Microstructure and crystallization behaviour of TiO<sub>2</sub> precursor prepared by the sol-gel method using metal alkoxide. *Journal of materials science*, 29, 1617-1622.

- Vitry, V., Francq, E., & Bonin, L. (2019). Mechanical properties of heat-treated duplex electroless nickel coatings. *Surface Engineering*, 35(2), 158-166.
- Vitry, V., Hastir, J., Mégret, A., Yazdani, S., Yunacti, M., & Bonin, L. (2022). Recent advances in electroless nickel boron coatings. *Surface and Coatings Technology*, 429, 127937.
- Vitry, V., Kanta, A. F., & Delaunois, F. (2012). Application of nitriding to electroless nickel–boron coatings: chemical and structural effects; mechanical characterization; corrosion resistance. *Materials & Design*, 39, 269-278.
- Wais, A. M. H., & Abid Ali, A. R. (2023, June). The Effect of Heat Treatment on Wear Properties of Ni-B-CNT Electroless Coating with Different Carbon Nanotube Concentration on AISI 4340 Steel. In *Materials Science Forum* (Vol. 1089, pp. 97-107). Trans Tech Publications Ltd.
- Yang, Y., Chen, W., Zhou, C., Xu, H., & Gao, W. (2011). Fabrication and characterization of electroless Ni–P–ZrO<sub>2</sub> nano-composite coatings. *Applied Nanoscience*, 1, 19-26.
- Yu, X., Zhao, G., Wang, F., & Wang, G. (1993). Catalytic Activities of Substrate Metals in a Ni–B–SiC Electroless Composite Bath. *Transactions of the Nonferrous Metals Society of China (China)*, 3(2), 36-40.
- Zhang, W. X., Jiang, Z. H., Li, G. Y., Jiang, Q., & Lian, J. S. (2008). Electroless Ni-P/Ni-B duplex coatings for improving the hardness and the corrosion resistance of AZ91D magnesium alloy. *Applied Surface Science*, 254(16), 4949-4955.
- Zhao, Q., Liu, Y., Müller-Steinhagen, H., & Liu, G. (2002). Graded Ni–P–PTFE coatings and their potential applications. *Surface and Coatings Technology*, 155(2-3), 279-284.
- Zhongcheng, G. U. O., Hongkang, L. I. U., Zhiyin, W. A. N. G., & Min, W. A. N. G. (1995). Process and properties of electroless plating RE-Ni-B-SiC composite coatings. *Acta Metallurgica Sinica (English Letters)*, 8(2), 118.

**International Journal**

Deviprasanna Mohanty, **Ajoy Kumar Bhowmick**, Tapan Kumar Barman, Prasanta Sahoo ,  
“Scratch and corrosion behaviour study of electroless Nickel-Boron(Ni-B) reinforced with  
ultrasonicated nano TiO<sub>2</sub>” Materials Today: Proceedings, 5 April 2023.

<https://doi.org/10.1016/j.matpr.2023.03.353>